POLITECNICO
MILANO 1863

Final Project: Multivariate Pricing

Financial Engineering - A.A. 2023-2024

Group Components:

Maspes Marco - CP: 10677441 - MAT: 216843
Tarditi Andrea - CP: 10728388 - MAT: 251722
Torba Matteo - CP: 10742071 - MAT: 252408

Contents

1 Introduction

In this project, we are introducing useful tools in order to price structured derivatives in the equity market.

From the paper Baviera & Azzone, 2021 we are exploiting the main passages of the synthetic forwards procedure: it is an alternative method to compute the values of discount factors and forwards prices from market prices of plain vanilla options.

Instead, from the paper Ballotta & Bonfiglioli, 2016 we are considering the explained model for the Multivariate Levy process in order to describe the forward dynamics over all the different possible maturities. The Levy model is compared to the Black model to better understand which are the strengths and the possible flaws of this new approach.

We will conclude in this paper that the Levy model is a useful pricing tool when dealing with multiple maturities and data from different markets since it correctly captures the volatility, whilst it could be more wise to use Black's model for a quicker and efficient estimation of the prices.

2 Forward Price martingality

Let's consider a 2 dimensional multivariate stochastic Levy process which describes the dynamic of a Forward Price, thus it takes consideration of the behaviour of the process in each available time step. The Levy process is described as the sum of multiple tempered alpha stable processes with their own distribution and dynamics; in the actual framework it is possible to identify precisely the structure of all these components:

Forward Price
$$F_i(t,T) = F_i(0,T) \cdot e^{X_i(t)+p_i \cdot t} \tag{1}$$

Levy process
$$X_i(t) = Y_i(t) + a_i \cdot Z(t) \tag{2}$$

Subordinated stable processes
$$\begin{aligned} Y_i(t) &= \beta_{Y_i} \cdot G(t) + \gamma_{Y_i} \cdot W(G(t)) \\ Z(t) &= \beta_Z \cdot G(t) + \gamma_Z \cdot W(G(t)) \end{aligned} \tag{3}$$

The structuring of a multivariate Levy process is an extremely important tool which can lead to a useful model describing the Forward prices. In order to build this model in a general framework, the main assumption made was about martingality: the use of a martingale process can eliminate completely the Levy drift term and consequently it simplifies the structure of the model. The martingale property needs to be fulfilled in the entire setting; the constant exponential term p_i was designed specifically to obtain the result.

Let's verify, step by step, the martingale property:

$$\begin{aligned} \mathbb{E}[F_i(t,T)|\mathcal{F}_0] &= \mathbb{E}[F_i(0,T) \cdot e^{X_i(t)+p_i \cdot t}|\mathcal{F}_0] = \\ &= \{since\ the\ F_i(0,T)\ is\ measurable\ with\ respect\ to\ the\ filtration\} = \\ &= F_i(0,T) \cdot \mathbb{E}[e^{X_i(t)+p_i \cdot t}|\mathcal{F}_0] = \\ &= \{assuming\ that\ the\ property\ is\ satisfied\} = \\ &= F_i(0,T) \end{aligned}$$

If the above property must be satisfied, it is necessary to assume the relation:

$$\mathbb{E}[e^{X_i(t)+p_i \cdot t}|\mathcal{F}_0] = 1$$

Assuming that p_i is a constant, $e^{p_i \cdot t}$ is a deterministic function and it can be taken out from the expectation, obtaining:

$$\mathbb{E}[e^{X_i(t)}|\mathcal{F}_0] = \mathbb{E}_0[e^{X_i(t)}] = e^{-p_i \cdot t}$$

It can be noticed that the drift compensator p_i can be written in terms of the characteristic function of X_i:

$$\Phi_{X_i}(-i;t) = e^{t\cdot\varphi(-i)} = \mathbb{E}_0\left[e^{i\cdot(-i)\cdot X_i}\right] = \mathbb{E}_0\left[e^{X_i}\right] = e^{-p_i\cdot t} \tag{4}$$

Up to this moment, the extensive formulation of the constant quantity p_i is unknown; in the following parts we will describe the characteristic function relation to obtain the final p_i structure.

2.1 Subordinated tempered alpha stable processes

The Levy process described in the previous paragraph is composed by multiple sub-parts, we assume they are distributed as tempered Normal Inverse Gaussian (NIG) and constructed as:

$$\begin{aligned} Y_i(t) &= \beta_{Y_i}\cdot G(t) + \gamma_{Y_i}\cdot W(G(t)) \quad \text{where } G(t)\sim IG(\nu_{Y_i}) \\ Z(t) &= \beta_Z\cdot G(t) + \gamma_Z\cdot W(G(t)) \quad \text{where } G(t)\sim IG(\nu_Z) \end{aligned}$$

The subordinator $G(t)$, which is distributed as an Inverse Gaussian, owns a specific formulation for its characteristic exponent. The characteristic function and the characteristic exponents are probabilistic tools that describe entirely the distribution of a random variable; they are based on an exponential construction that is different for each process:

Characteristic Function	$\Phi_X(u;t) = \mathbb{E}\left[e^{iu\cdot X_t(u)}\right] = e^{t\cdot\varphi_X(u)}$
Characteristic Exponent	$\varphi_X(u)$

The structure of the characteristic exponent of the subordinator $G(t)$ can be computed as:

$$\begin{aligned} \varphi_G(u) &= \frac{\alpha-1}{\alpha\cdot\nu}\left[\left(1-\frac{i\cdot u\cdot\nu}{1-\alpha}\right)^{\alpha}-1\right] = \left\{\textit{the IG model requires } \alpha=\frac{1}{2}\right\} = \\ &= \frac{1}{\nu}\cdot\left[1-\sqrt{1-2i\cdot u\cdot\nu}\right] \end{aligned}$$

However, it is necessary to insert this result into the general framework of NIG processes; exploiting the theoretical formulation of the subordinated motions it is possible to write the following relation:

$$\begin{aligned} \varphi_*(u) &= \varphi_G\big(u\cdot\beta_* + i\cdot u^2\cdot\frac{\gamma_*^2}{2}\big) \\ \Phi_*(u;t) &= e^{t\cdot\varphi_*(u)} \end{aligned}$$

Computing this formula for all the processes considered in the framework, we get the following characteristic exponents:

$$\varphi_{Y_j}(u) = \frac{1}{\nu_{Y_j}}\cdot\left[1-\sqrt{1-2i\cdot\nu_{Y_j}\cdot\left(\beta_{Y_j}\cdot u + i\cdot u^2\cdot\frac{\gamma_{Y_j}^2}{2}\right)}\right] = \frac{1}{\nu_{Y_j}}\cdot\left[1-\sqrt{1-2i\cdot\beta_{Y_j}\cdot u\cdot\nu_{Y_j}+\gamma_{Y_j}^2\cdot u^2\cdot\nu_{Y_j}}\right]$$

$$\varphi_Z(u) = \frac{1}{\nu_Z}\cdot\left[1-\sqrt{1-2i\cdot\nu_Z\cdot\left(\beta_Z\cdot u + i\cdot u^2\cdot\frac{\gamma_Z^2}{2}\right)}\right] = \frac{1}{\nu_Z}\cdot\left[1-\sqrt{1-2i\cdot\beta_Z\cdot u\cdot\nu_Z+\gamma_Z^2\cdot u^2\cdot\nu_Z}\right]$$

2.2 Characteristic function of a Levy process

The structure computed up to this moment only takes consideration of a singular NIG process, however the Levy process driving the Forward Price is the sum of multiple sub-processes and it's necessary to write its characteristic function. Following the structure generated by Ballotta and Bonfiglioli, 2016, we used the following formulation:

$$\begin{aligned}\Phi_{\mathbf{X}}(\mathbf{u};t) &= \Phi_Z\left(\sum_{j=1}^{n} a_j \cdot u_j; t\right)\prod_{j=1}^{n}\Phi_{Y_j}(u_j;t) = \\ &= \{\textit{considering the 2-dimensional case of our framework}\} \\ &= \Phi_Z(u_1\cdot a_1 + u_2\cdot a_2;t)\cdot\Phi_{Y_1}(u_1;t)\cdot\Phi_{Y_2}(u_2;t) = \\ &= e^{t\cdot\left(\frac{1}{\nu_Z}\cdot\left[1-\sqrt{1-2i\cdot\beta_Z\cdot(u_1a_1+u_2a_2)\cdot\nu_Z+\gamma_Z^2\cdot(u_1a_1+u_2a_2)^2\cdot\nu_Z}\right]\right)}\cdot e^{t\cdot\left(\frac{1}{\nu_{Y_1}}\cdot\left[1-\sqrt{1-2i\cdot\beta_{Y_1}\cdot u_1\cdot\nu_{Y_1}+\gamma_{Y_1}^2\cdot u_1^2\cdot\nu_{Y_1}}\right]\right)} \\ &\cdot e^{t\cdot\left(\frac{1}{\nu_{Y_2}}\cdot\left[1-\sqrt{1-2i\cdot\beta_{Y_2}\cdot u_2\cdot\nu_{Y_2}+\gamma_{Y_2}^2\cdot u_2^2\cdot\nu_{Y_2}}\right]\right)}\end{aligned}$$

From the multivariate formulation, the marginals' characteristic functions can be easily retrieved thanks to the properties of the multivariate characteristic function:

$$\begin{aligned}\Phi_{X_1}(u_1;t) &= \Phi_{\mathbf{X}}([u_1,0];t) \\ \Phi_{X_2}(u_2;t) &= \Phi_{\mathbf{X}}([0,u_2];t)\end{aligned}$$

$$\Phi_{X_j}(u_j;t) = e^{t\cdot\left(\frac{1}{\nu_{Y_j}}\cdot\left[1-\sqrt{1-2i\cdot u_j\cdot\nu_{Y_j}\cdot\beta_{Y_j}+u_j^2\cdot\gamma_{Y_j}^2\cdot\nu_{Y_j}}\right]+\frac{1}{\nu_Z}\cdot\left[1-\sqrt{1-2i\cdot u_i\ a_i\cdot\nu_Z\cdot\beta_Z+u_i^2\cdot a_i^2\cdot\gamma_Z^2\cdot\nu_Z}\right]\right)}$$

The distribution corresponding to this characteristic function is not immediately recognizable: we will understand it better in the upcoming section.

2.3 Marginal Convolution conditions

The marginal distribution of X_i has not been described yet as a known distribution, we can barely ansatz that it follows a NIG distribution but it is required to be proved theoretically. Let's assume the convolution conditions which relate the NIG processes Y_i with the Z common dependent term. They're two different conditions as expressed in the following formulation:

$$\begin{cases} k_i\cdot\theta_i &= \nu_Z\cdot a_i\cdot\beta_Z \\ k_i\cdot\sigma_i^2 &= \nu_Z\cdot a_i^2\cdot\gamma_Z^2 \end{cases} \tag{5}$$

The characteristic function of the previous Levy process can be modified exploiting these conditions:

$$\begin{aligned}\Phi_{X_i}(u_i) &= e^{t\cdot\left(\frac{1}{\nu_{Y_i}}\cdot\left[1-\sqrt{1-2i\cdot u_i\cdot\nu_{Y_i}\cdot\beta_{Y_i}+u_i^2\cdot\gamma_{Y_i}^2\cdot\nu_{Y_i}}\right]+\frac{1}{\nu_Z}\cdot\left[1-\sqrt{1-2i\cdot u_i\ a_i\cdot\nu_Z\cdot\beta_Z+u_i^2\cdot a_i^2\cdot\gamma_Z^2\cdot\nu_Z}\right]\right)} \\ &= e^{t\cdot\left(\frac{1}{\nu_{Y_i}}\cdot\left[1-\sqrt{1-2i\cdot u_i\cdot\nu_{Y_i}\cdot\beta_{Y_i}+u_i^2\cdot\gamma_{Y_i}^2\cdot\nu_{Y_i}}\right]+\frac{1}{\nu_Z}\cdot\left[1-\sqrt{1-2i\cdot u_i\cdot k_i\cdot\theta_i+u_i^2\cdot k_i\cdot\sigma_i^2}\right]\right)}\end{aligned}$$

The structure is still too specific to be considered the one of a NIG process, consequently we make another ansatz assuming that the quantities under the square roots are equal to each other and therefore can be grouped together. Due to the last decision, we are able to rewrite the characteristic function as:

$$\begin{aligned}\Phi_{X_i}(u_i) &= e^{t\cdot\left(\frac{1}{\nu_{Y_i}}+\frac{1}{\nu_Z}\right)\cdot\left[1-\sqrt{1-2i\cdot u_i\cdot k_i\cdot\theta_i+u_i^2\cdot k_i\cdot\sigma_i^2}\right]} = e^{t\cdot\left(\frac{\nu_{Y_i}+\nu_Z}{\nu_{Y_i}\cdot\nu_Z}\right)\cdot\left[1-\sqrt{1-2i\cdot u_i\cdot k_i\cdot\theta_i+u_i^2\cdot k_i\cdot\sigma_i^2}\right]} = \\ &= \left\{\textit{assuming that the quantity } \frac{\nu_{Y_i}\cdot\nu_Z}{\nu_{Y_i}+\nu_Z} = k_i\right\} = \\ &= e^{t\cdot\left(\frac{1}{k_i}\cdot\left[1-\sqrt{1-2i\cdot u_i\cdot k_i\cdot\theta_i+u_i^2\cdot k_i\cdot\sigma_i^2}\right]\right)}\end{aligned}$$

At this point, it is still required to prove that the previous square root equality holds. Using the following basic calculus procedure, we were able to succeed in the task:

$$\begin{aligned} 1-\sqrt{1-2i\cdot u\cdot \nu_{Y_i}\cdot \beta_{Y_i}+u^2\cdot \gamma_{Y_i}^2\cdot \nu_{Y_i}} &= 1-\sqrt{1-2i\cdot u\cdot k_i\cdot \theta_i+u^2\cdot k_i\cdot \sigma_i^2} \\ &\Updownarrow \\ 1-2i\cdot u\cdot \nu_{Y_i}\cdot \beta_{Y_i}+u^2\cdot \gamma_{Y_i}^2\cdot \nu_{Y_i} &= 1-2i\cdot u\cdot k_i\cdot \theta_i+u^2\cdot k_i\cdot \sigma_i^2 \\ &\Updownarrow \\ u\cdot \nu_{Y_i}\cdot \beta_{Y_i}+u^2\cdot \gamma_{Y_i}^2\cdot \nu_{Y_i} &= u\cdot k_i\cdot \theta_i+u^2\cdot k_i\cdot \sigma_i^2 \end{aligned}$$

Now it is possible to write a basic system with respect to the evaluation term $''u''$ in the previous equation:

$$\begin{cases} \nu_{Y_i}\cdot \beta_{Y_i}=k_i\cdot \theta_i \\ \gamma_{Y_i}^2\cdot \nu_{Y_i}=k_i\cdot \sigma_i^2 \end{cases} \tag{6}$$

Manipulating the structure of the system's equation, it is possible to get an extended description of the quantities θ_i and σ_i^2:

Derivation of θ_i:

$$\nu_{Y_i}=\frac{k_i\cdot \theta_i}{\beta_{Y_i}}=\{assuming\ the\ 1^{st}\ convolution\ condition\}=\frac{\nu_Z\cdot a_i\cdot \beta_Z}{\beta_{Y_i}}$$

$$\begin{aligned} \theta_i &= \frac{\nu_{Y_i}\cdot \beta_{Y_i}}{k_i}=\{inserting\ the\ k_i\ condition\}=\nu_{Y_i}\cdot \beta_{Y_i}\cdot\left(\frac{\nu_{Y_i}+\nu_Z}{\nu_{Y_i}\cdot \nu_Z}\right)=\{inserting\ the\ \nu_{Y_i}\ condition\}= \\ &= \beta_{Y_i}\cdot\frac{\nu_z\cdot\left(\frac{a_i\cdot \beta_z}{\beta_{Y_i}}+1\right)}{\nu_Z}=\beta_{Y_i}+a_i\cdot \beta_Z \end{aligned}$$

Derivation of σ_i^2:

$$\nu_{Y_i}=\frac{k_i\cdot \sigma_i^2}{\gamma_{Y_i}^2}=\{assuming\ the\ 2^{nd}\ convolution\ condition\}=\frac{\nu_Z\cdot a_i^2\cdot \gamma_Z^2}{\gamma_{Y_i}^2}$$

$$\begin{aligned} \sigma_i^2 &= \frac{\nu_{Y_i}\cdot \gamma_{Y_i}^2}{k_i}=\{inserting\ the\ k_i\ condition\}=\nu_{Y_i}\cdot \gamma_{Y_i}^2\cdot\left(\frac{\nu_{Y_i}+\nu_Z}{\nu_{Y_i}\cdot \nu_Z}\right)=\{inserting\ the\ \nu_{Y_i}\ condition\}= \\ &= \frac{\gamma_{Y_i}^2}{\nu_Z}\cdot \nu_Z\cdot\left(\frac{a_i^2\cdot \gamma_Z^2}{\gamma_{Y_i}^2}+1\right)=\gamma_{Y_i}^2+a_i^2\cdot \gamma_Z^2 \end{aligned}$$

As described above, associating these relations we were able to group together the square roots in our equation. Moreover it is possible to notice that the final form of the characteristic function of the Levy process resembles the form of a NIG distributed one:

$$\Phi_{X_i}(u_i)=e^{t\cdot\left(\frac{1}{k_i}\cdot\left[1-\sqrt{1-2i\cdot u_i\cdot k_i\cdot \theta_i+u_i^2\cdot k_i\cdot \sigma_i^2}\right]\right)}\sim NIG\left(\theta_i,\sigma_i^2,k_i\right) \tag{7}$$

Observation: The characteristic function found for X_i is the characteristic function for a NIG process proposed by Ballotta and Bonfiglioli, 2016, but it is slightly different from the formulation we have seen in class. Since the characteristic function uniquely defines the law of a random variable, we need to find the relationship between the parameters θ, σ and k of this formulation and the parameters η_C, σ_C and k_C of the formulation seen in class.

In class we defined the characteristic function of a NIG process as:

$$\mathcal{L}\left[\frac{u^2+i\cdot(1+2\cdot\eta_C)\cdot u}{2}\right] = e^{\frac{t}{k_C}\left(1-\sqrt{1+2\cdot\frac{u^2+i\cdot(1+2\cdot\eta_C)\cdot u}{2}\cdot k_C\cdot\sigma_C^2}\right)} = e^{\frac{t}{k_C}\left(1-\sqrt{1+2i\cdot u\cdot k_C\cdot(\frac{1}{2}+\eta_C)\cdot\sigma_C^2+u^2\cdot k_C\cdot\sigma_C^2}\right)}$$

In order to have the same expression found in (7), we need to impose that the coefficients of u and u^2 are the same. We end up with the following relationship among the model parameters:

$$k = k_C \qquad \theta = -\left(\frac{1}{2}+\eta_C\right)\cdot\sigma_C^2 \qquad \sigma = \sigma_C$$

2.4 Drift compensator

The last remaining step to compute explicitly the exponential term p_i is the evaluation of the marginal characteristic function in $u=-i$, since in equation (4) we had found:

$$\Phi_{X_i}(-i;t) = e^{t\cdot\varphi(-i)} = \mathbb{E}_0\left[e^{i\cdot(-i)\cdot X_i}\right] = \mathbb{E}_0\left[e^{X_i}\right] = e^{-p_i\cdot t}$$

Thus we can easily get the exponential drift compensator from the equation:

$$\begin{aligned} p_j &= -\varphi(u_j)|_{u_j=-i} = -\frac{1}{k_j}\cdot\left[1-\sqrt{1-2i\cdot u_j\cdot k_j\cdot\theta_j+u_j^2\cdot k_j\cdot\sigma_j^2}\,\right]|_{u=-i} = \\ &= -\frac{1}{k_j}\cdot\left[1-\sqrt{1-2\cdot k_j\cdot\theta_j-k_j\cdot\sigma_j^2}\,\right] \end{aligned} \tag{8}$$

3 Multivariate Levy constraints

The convolution conditions are useful for the computation of the characteristic function but they require too many parameters to be computed; then it is necessary to find an alternative formulation that simplifies and reduces the parameters used, keeping the dependence between processes.

We start by considering the 1^{st} convolution condition and we manage it:

$$k_i\cdot\theta_i = \nu_Z\cdot a_i\cdot\beta_Z \qquad \rightarrow \qquad a_i = \frac{k_i\cdot\theta_i}{\nu_Z\cdot\beta_Z} \qquad \rightarrow \qquad a_i^2 = \frac{k_i^2\cdot\theta_i^2}{\nu_Z^2\cdot\beta_Z^2}$$

Now we take consideration of the 2^{nd} convolution condition and plug in the previous relation obtained:

$$\begin{aligned} k_i\cdot\sigma_i^2 &= \nu_Z\cdot a_i^2\cdot\gamma_Z^2 = \{\textit{plugging in the previous relation}\} = \\ &= \nu_Z\cdot\frac{k_i^2\cdot\theta_i^2}{\nu_Z^2\cdot\beta_Z^2}\cdot\gamma_Z^2 = \frac{\gamma_Z^2}{\nu_Z\cdot\beta_Z^2}\cdot k_i^2\cdot\theta_i^2 \end{aligned}$$

Managing again the last relation, the convolution conditions collapse into a unique simplified relation:

$$k_i\cdot\sigma_i^2 = \frac{\gamma_Z^2}{\nu_Z\cdot\beta_Z^2}\cdot k_i^2\cdot\theta_i^2 \qquad \rightarrow \qquad \frac{\sigma_i^2}{k_i\cdot\theta_i^2} = \frac{\gamma_Z^2}{\nu_Z\cdot\beta_Z^2} = \text{ constant} = c \tag{9}$$

4 Linear correlation coefficient

The correlation coefficient is described in the following equation:

$$\rho^X_{1,2} = Corr(X_1(t), X_2(t)) = \frac{COV(X_1(t), X_2(t))}{\sqrt{\text{Var}[X_1(t)]} \cdot \sqrt{\text{Var}[X_2(t)]}} \tag{10}$$

In order to compute the linear correlation coefficient between the Levy processes $X_1(t)$ and $X_2(t)$, we can proceed in two different ways. The first possible approach is ignoring the fact that X_i is a NIG process and writing the variance of X_i in function of Y_i and Z. In the second approach, we use the fact that X_i is a NIG process (as proved in section 2.3).

4.1 First approach

In the first approach, we start by the definition of the covariance given by Ballotta and Bonfiglioli, 2016:

$$COV(X_1(t), X_2(t)) = a_1 \cdot a_2 \cdot Var[Z(1)] \cdot t \tag{11}$$

In order to compute the variances at the denominator of (10), we recall the definition of the m^{th} cumulant given in Ballotta and Bonfiglioli, 2016: for $i = 1, \dots, n$, the m^{th} cumulant, c_m, of the i^{th} component of $X(t)$ is

$$c_m(X_i(t)) = t[c_m(Y_i(1)) + a_i^m c_m(Z(1))]$$

This formula can be used to compute the variance of X_i obtaining:

$$Var[X_i(t)] = t \cdot [Var[Y_i(1)] + a_i^2 \cdot Var[Z(1)]] \tag{12}$$

For every process U having a NIG distrubution, using the subordinated relations described in the book Cont and Tankov, 2004, we have:

$$U \sim NIG(\beta_U, \gamma_U^2, \nu_U) \qquad \rightarrow \qquad \text{Var}[U(t)] = \gamma_U^2 \cdot t + \beta_U^2 \cdot \nu_U \cdot t$$

Since we assume that Y_i and Z have NIG distributions, we can write:

$$Var[Y_i(1)] = \gamma_i^2 + \beta_i^2 \cdot \nu_i \qquad \text{for } i = 1, 2 \tag{13}$$

$$Var[Z(1)] = \gamma_Z^2 + \beta_Z^2 \cdot \nu_Z \tag{14}$$

By substitution of (14) in (11), and by further simplifications we get:

$$\begin{aligned} COV(X_1(t), X_2(t)) &= a_1 \cdot a_2 \cdot (\gamma_Z^2 + \beta_Z^2 \cdot \nu_Z) \cdot t = a_1 \cdot a_2 \cdot \gamma_Z^2 \cdot \left(1 + \frac{\beta_Z^2 \cdot \nu_Z}{\gamma_Z^2}\right) \cdot t = \\ &= \{\textit{using the expression found in } (9)\} = \\ &= a_1 \cdot a_2 \cdot \gamma_Z^2 \cdot \left(1 + \frac{1}{c}\right) \cdot t \end{aligned} \tag{15}$$

By plugging (13) and (14) in (12), and by proceeding with the computations, we obtain:

$$\begin{aligned}
Var[X_i(t)] &= t \cdot [(\gamma_i^2 + \beta_i^2 \cdot \nu_i) + a_i^2 \cdot (\gamma_Z^2 + \beta_Z^2 \cdot \nu_Z)] = \\
&= t \cdot \left\{ \frac{1}{\nu_i} \cdot [\nu_i \cdot \gamma_i^2 + \beta_i^2 \cdot \nu_i^2] + a_i^2 \cdot \gamma_Z^2 \cdot \left[1 + \frac{\beta_Z^2 \cdot \nu_Z}{\gamma_Z^2} \right] \right\} = \\
&= \{ \textit{using the relationships found in (6)} \} = \\
&= t \cdot \left\{ \frac{1}{\nu_i} \cdot [k_i \cdot \sigma_i^2 + k_i^2 \cdot \theta_i^2] + a_i^2 \cdot \gamma_Z^2 \cdot \left[1 + \frac{\beta_Z^2 \cdot \nu_Z}{\gamma_Z^2} \right] \right\} = \\
&= t \cdot \left\{ \frac{k_i \cdot \sigma_i^2}{\nu_i} \cdot \left[1 + \frac{k_i \cdot \theta_i^2}{\sigma_i^2} \right] + a_i^2 \cdot \gamma_Z^2 \cdot \left[1 + \frac{\beta_Z^2 \cdot \nu_Z}{\gamma_Z^2} \right] \right\} = \\
&= \{ \textit{using the expression found in (9)} \} = \\
&= t \cdot \left\{ \frac{k_i \cdot \sigma_i^2}{\nu_i} \cdot \left[1 + \frac{1}{c} \right] + a_i^2 \cdot \gamma_Z^2 \cdot \left[1 + \frac{1}{c} \right] \right\} = \\
&= t \cdot \left[1 + \frac{1}{c} \right] \cdot \left\{ \frac{k_i \cdot \sigma_i^2}{\nu_i} + a_i^2 \cdot \gamma_Z^2 \right\}
\end{aligned} \tag{16}$$

At this point, we can substitute the expressions (15) and (16) in the expression of the covariance reported in 10) and proceed with the simplifications:

$$\begin{aligned}
\rho_{1,2}^X &= \frac{COV(X_1(t), X_2(t))}{\sqrt{\mathrm{Var}[X_1(1)]} \cdot \sqrt{\mathrm{Var}[X_2(1)]}} = \\
&= \frac{a_1 \cdot a_2 \cdot \gamma_Z^2 \cdot \left(1 + \frac{1}{c} \right) \cdot t}{\sqrt{t \cdot \left(1 + \frac{1}{c} \right) \cdot \left(\frac{k_1 \cdot \sigma_1^2}{\nu_1} + a_1^2 \cdot \gamma_Z^2 \right)} \cdot \sqrt{t \cdot \left(1 + \frac{1}{c} \right) \cdot \left(\frac{k_2 \cdot \sigma_2^2}{\nu_2} + a_2^2 \cdot \gamma_Z^2 \right)}} = \\
&= \frac{a_1 \cdot a_2 \cdot \gamma_Z^2}{\sqrt{\frac{k_1 \cdot \sigma_1^2}{\nu_1} + a_1^2 \cdot \gamma_Z^2} \cdot \sqrt{\frac{k_2 \cdot \sigma_2^2}{\nu_2} + a_2^2 \cdot \gamma_Z^2}} = \{ \textit{using the second relationship found in (6)} \} = \\
&= \frac{a_1 \cdot a_2 \cdot \gamma_Z^2}{\sqrt{\gamma_1^2 + a_1^2 \cdot \gamma_Z^2} \cdot \sqrt{\gamma_2^2 + a_2^2 \cdot \gamma_Z^2}} = \{ \textit{using the convolution conditions} \} = \\
&= \frac{a_1 \cdot a_2 \cdot \gamma_Z^2}{\sigma_1 \cdot \sigma_2} = \{ \textit{substituting the values of } \sigma_1 \ \& \ \sigma_2 \} = \\
&= \sqrt{k_1 \cdot k_2} \cdot \frac{a_1 \cdot a_2 \cdot \gamma_z^2}{\nu_Z \cdot \gamma_Z^2 \cdot a_1 \cdot a_2} = \frac{\sqrt{k_1 \cdot k_2}}{\nu_Z}
\end{aligned} \tag{17}$$

4.2 Second approach

The linear correlation coefficient between the marginals X_i can be computed also in the case in which we assume the NIG distribution of the X_i.

The starting correlation coefficient formulation, given also by Ballotta and Bonfiglioli, 2016, is described in the following equation, in which the dependence from time has been already simplified:

$$\rho_{1,2}^X = \frac{a_1 \cdot a_2 \cdot \mathrm{Var}[Z(1)]}{\sqrt{\mathrm{Var}[X_1(1)]} \cdot \sqrt{\mathrm{Var}[X_2(1)]}} \tag{18}$$

Consequently, in our framework, we can easily evaluate our NIG processes variances:

$$\begin{aligned}\text{Var}[Z(1)] &= \gamma_Z^2 + \beta_Z^2 \cdot \nu_Z \\ \text{Var}[X_1(1)] &= \sigma_1^2 + \theta_1^2 \cdot k_1 \\ \text{Var}[X_2(1)] &= \sigma_2^2 + \theta_2^2 \cdot k_2\end{aligned}$$

Then, the starting relation, given in (18), is described in the following equation:

$$\rho_{1,2}^X = \frac{a_1 \cdot a_2 \cdot \text{Var}[Z(1)]}{\sqrt{\text{Var}[X_1(1)]} \cdot \sqrt{\text{Var}[X_2(1)]}} = \frac{a_1 \cdot a_2 \cdot \left(\gamma_Z^2 + \beta_Z^2 \cdot \nu_Z\right)}{\sqrt{\sigma_1^2 + \theta_1^2 \cdot k_1} \cdot \sqrt{\sigma_2^2 + \theta_2^2 \cdot k_2}}$$

The initial description of the linear correlation coefficient requires to use too many parameter that should be calibrated, then it is better to reduce the structure of the coefficient in order to simplify its expression for the calibration:

$$\begin{aligned}\rho_{1,2}^X &= \frac{a_1 \cdot a_2 \cdot \left(\gamma_Z^2 + \beta_Z^2 \cdot \nu_Z\right)}{\sqrt{\sigma_1^2 + \theta_1^2 \cdot k_1} \cdot \sqrt{\sigma_2^2 + \theta_2^2 \cdot k_2}} = \frac{a_1 \cdot a_2 \cdot \left(\gamma_Z^2 + \beta_Z^2 \cdot \nu_Z\right)}{\sigma_1 \cdot \sigma_2 \cdot \sqrt{1 + \frac{\theta_1^2 \cdot k_1}{\sigma_1^2}} \cdot \sqrt{1 + \frac{\theta_2^2 \cdot k_2}{\sigma_2^2}}} = \\ &= \frac{a_1 \cdot a_2 \cdot \left(\gamma_Z^2 + \beta_Z^2 \cdot \nu_Z\right)}{\sigma_1 \cdot \sigma_2 \cdot \left(1 + \frac{1}{c}\right)} = \left\{\textit{substituting the real value of } c\right\} = \\ &= \frac{a_1 \cdot a_2 \cdot \gamma_Z^2 \left(\gamma_Z^2 + \beta_Z^2 \cdot \nu_Z\right)}{\sigma_1 \cdot \sigma_2 \cdot \left(\gamma_Z^2 + \beta_Z^2 \cdot \nu_Z\right)} = \frac{a_1 \cdot a_2 \cdot \gamma_z^2}{\sigma_1 \cdot \sigma_2} = \\ &= \left\{\textit{substituting the values of } \sigma_1 \ \& \ \sigma_2\right\} = \sqrt{k_1 \cdot k_2} \cdot \frac{a_1 \cdot a_2 \cdot \gamma_z^2}{\nu_Z \cdot \gamma_Z^2 \cdot a_1 \cdot a_2} = \frac{\sqrt{k_1 \cdot k_2}}{\nu_Z}\end{aligned} \tag{19}$$

As we expected, with this alternative method the correlation coefficient expression found is equal to the one found in (17).

4.3 Correlation bounds

Up to this moment, we have not studied yet the lower and upper bound correlation coefficient related to the multivariate process. The lower bound is easy to describe: since all the terms are strictly positive the correlation coefficient $\rho_{1,2}^X$ could decrease only till 0, thus it can solely represent the *positive correlation framework* of the markets.

The upper bound however should be proved again by hand from the previous equation. We need to go back in the initial singular NIG parameters in order to find a satisfying formulation:

$$\begin{aligned}\rho_{1,2}^X &= \frac{\sqrt{k_1 \cdot k_2}}{\nu_Z} = \left\{\textit{substituting the values of } k_1 \ \& \ k_2 \textit{ from the convolution conditions}\right\} = \\ &= \frac{1}{\nu_Z} \cdot \sqrt{\frac{\nu_Z^2 \cdot \nu_1 \cdot \nu_2}{(\nu_1 + \nu_Z) \cdot (\nu_2 + \nu_Z)}} = \sqrt{\frac{\nu_1 \cdot \nu_2}{(\nu_1 + \nu_Z) \cdot (\nu_2 + \nu_Z)}} \quad \xrightarrow{\nu_Z \to 0} \quad 1\end{aligned}$$

Thus the only parameter which controls the correlation coefficients is the parameter ν_Z: the lower it is, the nearer to 1 is the correlation coefficient.

4.4 Financial interpretation

Globalization has profoundly transformed world economies, creating an environment where financial markets are closely correlated. This interdependence is particularly evident between the U.S. and European stock markets, represented respectively by the S&P 500 and the EUROSTOXX50. Multinational corporations operating in both regions influence each other's economic conditions, creating synchronized financial results and consequently, stock market movements.

Monetary policies of central banks, such as the Federal Reserve and the European Central Bank, show significant convergence, especially in response to global crises. Synchronized interest rates and economic stimulus programs have simultaneous effects on the stock markets of both regions, reinforcing the correlation between the S&P 500 and the EUROSTOXX50.

We can conclude saying that EU and USA markets are deeply correlated due to geopolitical conditions, monetary policies and enlargement of the boundaries in which investors tend to operate.

5 Forwards creation

The main driver of the **multivariate exponential Levy** pricing was to exploit and discover a new method in order to price correctly the Plain Vanilla options. It could be difficult to apply the same reasoning to exotic options due to the strange and complex structure of their payoff.

The term structure is a key ingredient in the derivative market since it is used to derive the discount rates for expected payoffs. As a general statement it is possible to affirm that **interest rates used for derivative pricing are not risk free** since they should depend on the risks implied in the investment. If we take into consideration exchange-traded derivatives the presence of a clearing house grants the possibility of neglecting default risk of the market participants.

Previously the obvious choice was to take into consideration the Libor curve as the discounting term structure but, after the great **financial crisis of 2007** and the latest flactuations in the market, the difference in tenor of the Libor curve has enlarged to several basis points.

The **Overnight Index Swap (OIS) curve**, swap derived from the inter-bank overnight rate, has therefore emerged as a natural substitute of the previous term structure for risk-free derivative discounting due to its high liquidity. Considering a market maker's point of view the use of OIS curve to derive discount factors allows to represents other risks and costs not included in the risk free rate.

The objective of the following procedure is to use the Put/Call parity relation in order to price a discount factor and a Forward instrument that can **overtake the bootstrap procedure**.

5.1 Methodology

Let's introduce the framework in which we will work; we consider Plain Vanilla Call and Put options exchanged on the EURO STOXX 50 and the S&P 500, respectively the most liquid equity index in the Euro area and in the U.S.A. Both the datasets contain different maturities, options prices and market implied volatilities.
The procedure that will lead to the Forwards creation is composed by a few key steps:

- The **Synthetic Forwards procedure** tries to exploit the market information without necessarily computing a Bootstrap to obtain the rates.
- Therefore it is necessary to find an alternative method to compute the **discount factors**, key element of the financial modelling.
- The last step is the computation of the **Forward price**; exploiting the Put/Call parity relation from Black model it is possible to obtain the required value with little work.

5.2 Synthetic Forwards

Now let's dive into a more detailed explanation for this forward instruments.

Synthetic Forwards are tool that can be computed directly from the market prices of Call and Put options, it is used to simplify the pricing procedure and nowadays they are able to represent the post crisis framework in a precise manner.

The Synthetic Forwards, for sake of notation we will call them SF from now on, are build upon two different indexes: the SF Bid and the SF Ask, that can be computed in the following way:

$$\begin{cases} \mathscr{G}^{\text{bid}}(K) & = C^{\text{bid}}(K) - P^{\text{ask}}(K) \\ \mathscr{G}^{\text{ask}}(K) & = C^{\text{ask}}(K) - P^{\text{bid}}(K) \end{cases}$$

Consequently it's possible to compute the general version of the synthetic forwards as:

$$\mathscr{G}(K) = \frac{\mathscr{G}^{\text{bid}}(K) + \mathscr{G}^{\text{ask}}(K)}{2}$$

5.3 Constructed discount factor

The creation of the Forward prices necessitates a discount factor to be computed; however, without the Bootstrap procedure, it is necessary to generate a synthetic discount factor called $\bar{B}(t_0, T)$ which can carry the overall computation. Obviously, we will require one different discount factor for each maturity that we are considering.

The computation of the synthetic discount factor is quite simple and can be obtained via the least square estimation:

$$\overline{B}(t_0, T) = -\frac{\sum_{i=1}^{N}(K_i - \hat{K}) \cdot (\mathscr{G}(K_i) - \hat{\mathscr{G}})}{\sum_{i=1}^{N}(K_i - \hat{K})^2} \tag{20}$$

where

$$\hat{\mathscr{G}} = \frac{1}{N}\sum_{i=1}^{N}\mathscr{G}(K_i) \text{ is the mean Synthetic Forward} \qquad \hat{K} = \frac{1}{N}\sum_{i=1}^{N}K_i \text{ is the mean strike}$$

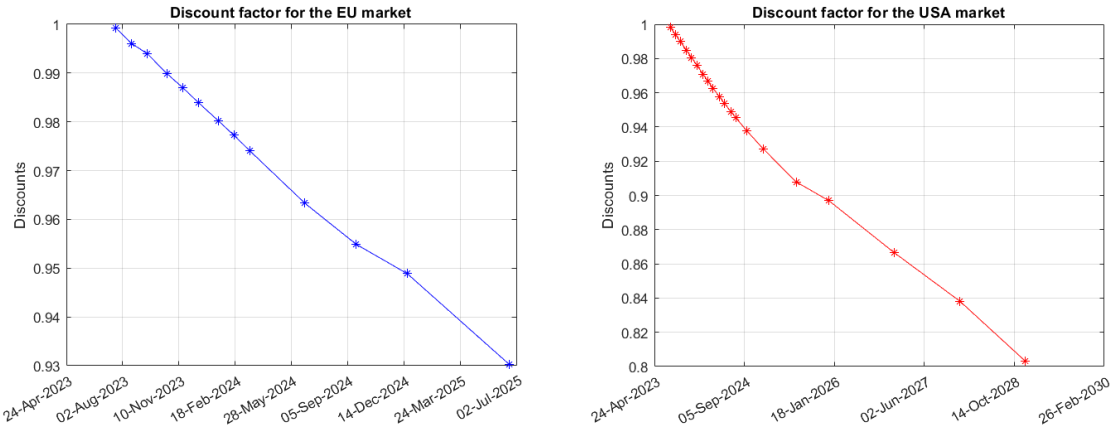

(1a) (1b)

Figure 1: Market discounts obtained from the quoted prices of Plain Vanilla options via the synthetic forwards procedure for the EU market (1a) and for the USA market (1b).

The above plots show the behaviour of the discounts; it can be seen that the pattern is particular since instead of a curve we got almost a straight line with no curvature.

5.4 Forward prices

The forward price is the final goal required from the procedure, therefore the discount factor should be related in a statistical way to the real Forward. This relation can be obtained through the exploitation of the Black Put/Call parity relation:

$$\textbf{Put/Call parity} \qquad C(K) - P(K) = B(t_0, T) \cdot [F(t_0, T) - K]$$

In our framework we are not able to compute directly all the quantities required but we need to approximate them from the market, as the previous steps show. Therefore the Put/Call parity can be transformed in an empirical formula:

$$C_{mkt}(K) - P_{mkt}(K) = \bar{B}(t_0, T) \cdot [F(t_0, T) - K] + \epsilon_i = \mathscr{G}(K)$$

The initial forward price can be consequently obtained inverting the equation:

$$F(t_0, T) = \frac{\mathscr{G}(K)}{\bar{B}(t_0, T)} + K \tag{21}$$

It's necessary to recall that the final formula of the forwards should theoretically overtake the bootstrap one, however we neglect the noise term ϵ_i in the computation.

Due to the AoA principle, the forward F should be constant in K, however, since the market discounts $\bar{B}(t_0, T)$ are obtained via the least square estimation expressed in (20), the values of F make some small oscillations over the whole set of strikes at each fixed maturity: in order to tackle this problem and to have a unique arbitrage-free forward price for the upcoming sections, we decided to compute the mean forward price across the different strikes at each maturity.

Moreover, from our results, we can observe that $\frac{\mathscr{G}(K)}{\bar{B}(t_0,T)}$ is a decreasing linear function of K with angular coefficient -1, whose absolute value is a limit of the slope. This fits correctly with the theoretical guidelines which require the coefficient of $\frac{\mathscr{G}(K)}{\bar{B}(t_0,T)}$, real bootstrapped version of our framework, to be lower in absolute value of 1.

The forwards can own multiple behaviours depending on the maturity and market considered; here the plots show a small amount of the results explained in **Appendix 2**.

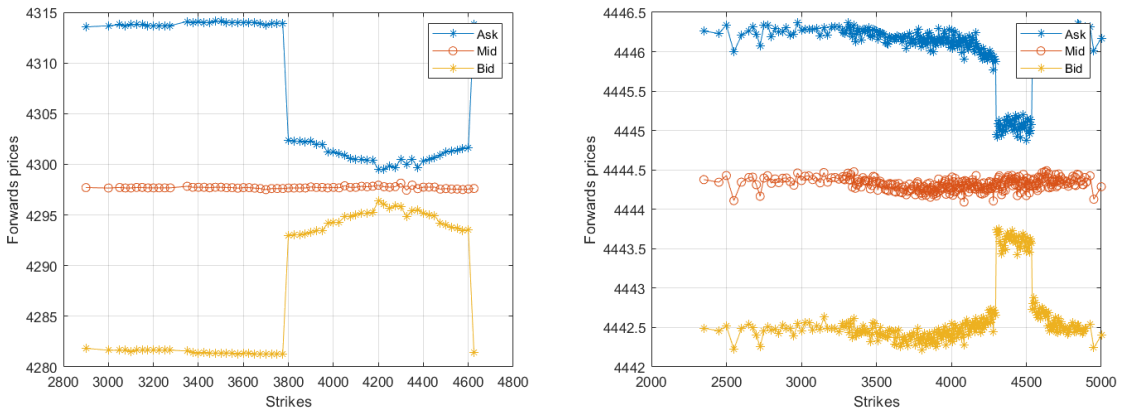

(2a) (2b)

Figure 2: Forwards obtained via the synthetic forwards procedure for the EU market (2a) and the USA market (2b).

As the previous plots show, the American market is more unstable than the European one; the higher volatility of the contracts is the cause of this fluctuations.

6 Multivariate Levy model calibration

The multivariate Levy processes introduced in (2) and the market implied forward prices F obtained in the previous section are useful tools to build a model and calibrate it using the market prices.

Consider the forward prices of the assets describing the S&P500 and the EUROSTOOXX50 indices, and assume that their dynamics is of the form:

$$F_i(t,T) = F_i(0,T) \cdot e^{X_i(t)+p_i \cdot t} \text{ for } i = 1,2$$

Notation: From now on the pedix 1 refers to the USA market, while the pedix 2 refers to the European one.

In the forward exponent, p_i is the drift compensator obtained in Section 2.4, while X_i is described by two multivariate Levy processes of the form: $X_i(t) = Y_i(t) + a_i \cdot Z(t)$ for $i = 1,2$ where $Y_i(t)$ and $Z(t)$ are NIG processes.

The **purpose of this section** is to calibrate a model in order to compute the prices of European Plain Vanilla Options on the S&P500 and the EUROSTOOXX50 indices.

The main steps that will lead to the final choice of calibrated parameters can be described as:

- The **market data** on European Call and Put Options are **refined** to have a more reliable calibration dataset.
- The first half of the procedure exploit a **Joint calibration** of the marginal parameters of the NIG processes, using the selected Put and Call prices as suggested by Ballotta and Bonfiglioli, 2016.
- The second half tries to calibrate the parameters of the idiosyncratic processes (i.e. $Y_i(t)$), and the systematic component (i.e. $Z(t)$), by fitting the correlation using Least Squares method.

Finally, this section is concluded by an analysis of the goodness of the calibrated model.

6.1 Refinement of the dataset

We start by the dataset explained in **Appendix 1** containing the market prices of European Call and Put Options on the S&P500 and the EUROSTOOXX50 indices for several expires and strike prices. The dataset at this point cannot be used in order to calibrate a complex model as the Levy framework, therefore it is necessary to choose and refine the structures according to two main criteria.

The first criteria tries to highlight only the stochastic component of the option prices avoiding the initial Spot to be too determinant in the final value; moreover we decide to keep only the OTM options to ensure that the most liquid products are chosen to represent the maturity.

The second criteria is related to filtering out the options with $|\Delta_{Black\&Scholes}| \notin [10\%, 90\%]$: this allows to consider OTM options which are not too far from the ATM ones.

Since the model aims at having a good representation of the market implied volatilities, we compute them from the OTM options' market prices through the Black formula and we represent graphically the related volatilities smiles over the different expires, hoping for a smooth behaviour of the curves. In general, we obtain very good results, as it can be observed in the following plots.

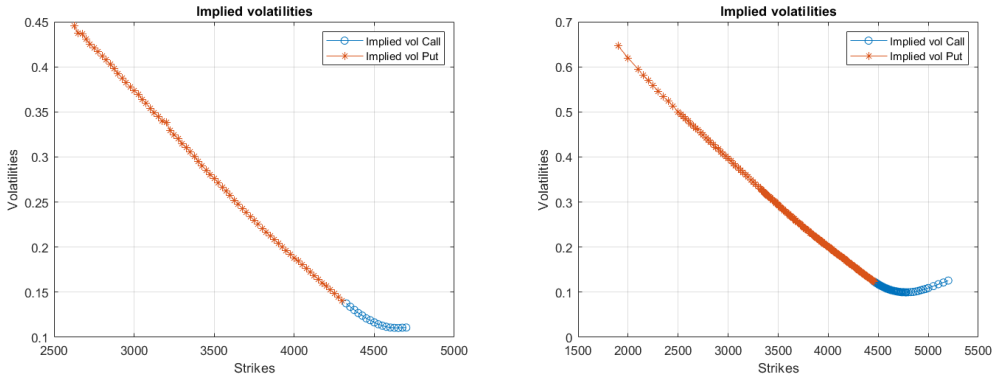

(3a) (3b)

Figure 3: Implied volatilities computed from the quoted OTM options' prices with Expiry 15-Sep-2023 for the European market (3a) and for the American Market (3b).

Unfortunately, for the last American expiry the result is not as good as in the other cases and the volatility smile presents some irregularities, as can be appreciated in Figure (4a).

The first approach to tackle this problem, is to consider only the market prices of the call options and compute the corresponding put prices via put-call parity to fill the left hand of the curve: however, this methodology is not resolutive since the implied volatility smile behaviour remains similar.

Another possible solution is to remove the options corresponding to the irregularities of the curve: thanks to this approach we are able to obtain a smooth smile as represented in Figure (4b). However, we keep our attention on this maturity and we try to understand if it has an influence in the calibration process.

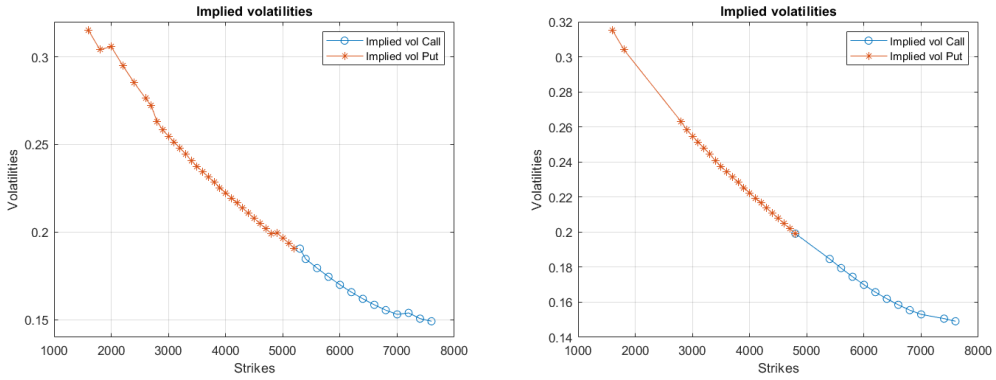

(4a) (4b)

Figure 4: Implied volatilities computed from the quoted OTM options' prices with Expiry 15-Dec-2028 for the American Market before (4a) and after (4b) removing some "problematic" prices to smoothen the implied volatility smile.

To further refine the dataset, we try to understand whether all the maturities are relevant for our calibration, and if the presence of some outliers worsen the calibration process. As better explained in the **Appendix 3**, using a multi calibration procedure we deduce that, as previously suspected, the last American maturity can highly worsen the marginal parameters calibration.

6.2 Joint calibration

The aim of this section is to jointly calibrate the set of parameters $\mathscr{P} = \{\kappa_1, \theta_1, \sigma_1, \kappa_2, \theta_2, \sigma_2\}$ that represent the marginal NIG processes $X_1 \sim NIG(\kappa_1, \sigma_1^2, \theta_1)$ and $X_2 \sim NIG(\kappa_2, \sigma_2^2, \theta_2)$ related by the constraint retrieved in Section 3:

$$\frac{\sigma_1^2}{\theta_1^2 \cdot \kappa_1} = \frac{\sigma_2^2}{\theta_2^2 \cdot \kappa_2} = constant$$

Using the refined dataset of Plain Vanilla options presented in the previous section, the parameters can be obtained by minimizing the following objective function:

$$\Theta = \arg\min_{\mathscr{P}} \quad w_{EU} \cdot RMSE_{EU} + w_{USA} \cdot RMSE_{USA} \tag{22}$$

The choice of the weights can be made to balance the different value of the spot in the two markets, by selecting:

$$w_{EU} = \frac{S_{EU}(0)}{S_{EU}(0) + S_{USA}(0)} \qquad w_{USA} = \frac{S_{USA}(0)}{S_{EU}(0) + S_{USA}(0)} \tag{23}$$

The RMSE is computed as:

$$RMSE = \sum_{t=1}^{T} \sqrt{\frac{\sum_{j:K_j<F_t} \left(P_{tj}^{MKT} - P_{tj}^{MODEL}\right)^2 + \sum_{j:K_j>F_t} \left(C_{tj}^{MKT} - C_{tj}^{MODEL}\right)^2}{N_{options}}} \tag{24}$$

where P_{tj}^{MKT} and C_{tj}^{MKT} are the market prices of the Put and Call options, $N_{options}$ is the total number of options considered for each maturity, C_{tj}^{MODEL} and P_{tj}^{MODEL} are the model Plain Vanilla prices and they depend on the calibrated parameters.

In the Multivariate Levy model, the call prices are computed via the Lewis formula; given a log-moneyness grid x, the price of the corresponding call option is given by:

$$C(x)^{MODEL} = \bar{B}(0,t) \cdot F(0,t) \cdot \left(1 - e^{-\frac{x}{2}} \cdot \int_{-\infty}^{\infty} \frac{d\xi}{2\pi} \cdot e^{-i\xi x} \cdot \phi\left(-\xi - \frac{i}{2}\right) \cdot \frac{1}{\xi^2 + \frac{1}{4}}\right) \tag{25}$$

where $\phi_j(\xi) = e^{t \cdot \left(\frac{1}{\kappa_j} \cdot \left[1 - \sqrt{1 - 2i \cdot \xi \cdot \kappa_j \cdot \theta_j + \xi^2 \cdot \kappa_j \cdot \sigma_j^2}\right] + i \cdot \xi \cdot p_j\right)}$
where p_j is the drift compensator found in Section 2.4

In this expression, to determine the market discount and the forward price, we used the values of $\bar{B}(0,t)$ and $F(0,t)$ obtained via the synthetic forwards procedure illustrated in Section 2.4, according to the results of Azzone and Baviera, 2021.

The Fourier transform inside the Lewis expression can be computed through a FFT approach: this allows us to simplify the integral form resolution with respect to other computational techniques (e.g. quadrature methods), since we can parallelize the integral computation over different strike prices.

The FFT parameters are selected accordingly to the suggested theory, choosing a number of intervals equal to 2^{15} and a step in the moneyness grid as $dz = 0.001$: this choice is made by seeking for a trade off between the exactness of the results and the computational time.

Once the call prices are computed, the corresponding Put option prices P_{tj}^{MODEL} are retrieved via the Put-Call parity:

$$P_{tj}^{MODEL} = C_{tj}^{MODEL} - \bar{B}(0,t) \cdot (F(0,t) - K_j) \tag{26}$$

using again the values of $\bar{B}(0,t)$ and $F(0,t)$ obtained in Section 5.

The calibrated parameters obtained from the joint calibration procedure are the ones reported in the following table:

	USA	EU
k	3.8295	0.8259
θ	-0.0941	-0.1621
σ	0.1558	0.1246
(w)RMSE	119.2546	

Table 1: Calibrated marginal parameters for X_1 and X_2 and objective function value.

As we expected from previous considerations over the general structure of the S&P500 and the EUROSTOXX50 indexes, the American volatility is higher; this can also justify the greater volvol value for the American market. The negative values of the skewness for both the indexes could have been forecast from the market implied volatilities smiles plotted in the previous section.

6.3 Idiosyncratic and Systematic calibration

The second step of the calibration tries to exploit the market correlation and the convolution conditions in order to define the parameters of the idiosyncratic and the systematic processes.

We proceed by calibrating the value of ν_1, ν_2 and ν_Z at first and the values of the other parameters are obtained following the theoretical relations among them.

The objective function created to calibrate the three ν is the following:

$$\Psi = \arg \min_{\nu_1,\nu_2,\nu_Z} \quad \left(\rho^{MODEL} - \rho^{MKT}\right)^2 \tag{27}$$

where ρ^{MKT} is the historical correlation computed from the yearly returns of the S&P500 and the EUROSTOXX50 indices, while the correlation of the model is $\rho^{MODEL} = \sqrt{\frac{\nu_1 \cdot \nu_2}{(\nu_1+\nu_Z)\cdot(\nu_2+\nu_Z)}}$, as found in (19).

The minimization problem is solved under the following constraints:

$$\begin{cases} \frac{\nu_1 \cdot \nu_Z}{(\nu_1+\nu_Z)} & = k_1 \\ \frac{\nu_2 \cdot \nu_Z}{(\nu_2+\nu_Z)} & = k_2 \\ \frac{\nu_1 \cdot \nu_2}{(\nu_1+\nu_Z)\cdot(\nu_2+\nu_Z)} & = \frac{k_1 \cdot k_2}{\nu_Z^2} \\ \nu_i > 0 & \text{for } i = 1, 2, Z \end{cases}$$

The values of the calibrated parameters are described in the following table:

ν_1	ν_2	ν_Z
10.2638	0.9550	6.1087

Table 2: Calibrated dependence parameters

Financial Interpretation

Coherently to previous results, the volvol of the American idiosyncratic component is notably higher than the European one, the second question is always: why?

Calibrating across multiple maturities and two datasets regarding different markets, as we expected, yields high value's of " vol o vol" due to the large number of maturities that need to be considered. Even thought our

model capture's correctly the volatility and yields us accurate prices and vols adherent with the market once it would be a bald statement if we said that we are completely satisfied with the $\nu's$ obtained.

This is a limit in our model that relays on algorithms that don't have the power to escape from a local minimum when treating a large dataset: The model yields results that satisfy our constraints, price correctly and capture the volatility slope but computes a set of parameter that we are not able to fully interpret in a standard market framework.

Using the calibrated values of the marginal parameters and of ν_1, ν_2 and ν_z, the other idiosyncratic and systematic parameters can be retrieved. Form the convolutions conditions expressed in (5), taken from Ballotta and Bonfiglioli, 2016, we can compute the values of a_1, a_2, γ_z and β_z by solving the following system:

$$\begin{cases} a_1 \cdot \beta_z &= \frac{k_1 \cdot \theta_1}{\nu_z} \\ a_2 \cdot \beta_z &= \frac{k_2 \cdot \theta_2}{\nu_z} \\ k_1 \cdot \sigma_1^2 &= \nu_z \cdot a_1^2 \cdot \gamma_z^2 \\ k_2 \cdot \sigma_2^2 &= \nu_z \cdot a_2^2 \cdot \gamma_z^2 \end{cases}$$

Finally, the remaining parameters are calibrated by exploiting the conditions in (10) of Ballotta and Bonfiglioli, 2016: for $i = 1, 2$ we compute the parameters as

$$\beta_i = \theta_i - a_i \cdot \beta_z$$
$$\gamma_i = \sqrt{\sigma_i^2 - a_i^2 \cdot \gamma_z^2}$$

A summary table with all the calibrated parameters is reported below:

	k	θ	σ
USA	3.8295	-0.0941	0.1558
EU	0.8259	-0.1621	0.1246

Table 3: Calibrated parameters for X.

	ν	β	γ
USA	10.2638	-0.0351	0.0952
EU	0.9550	-0.1402	0.1159

Table 4: Calibrated parameters for Y.

	ν	β	γ	a_{USA}	a_{EU}
Z	6.1087	0.5776	1.2072	-0.1022	-0.0379

Table 5: Calibrated parameters for Z.

6.4 Analysis of the calibrated Levy model

Exploring these results through a graphic method, we plot the implied volatility's computed via the model with the calibrated parameters for all the available market data: we do this by computing the Levy model prices through the Lewis formula, and we retrieve the Black implied volatilities. The following examples can be used to better interpret the fitting of our parameters:

American market:

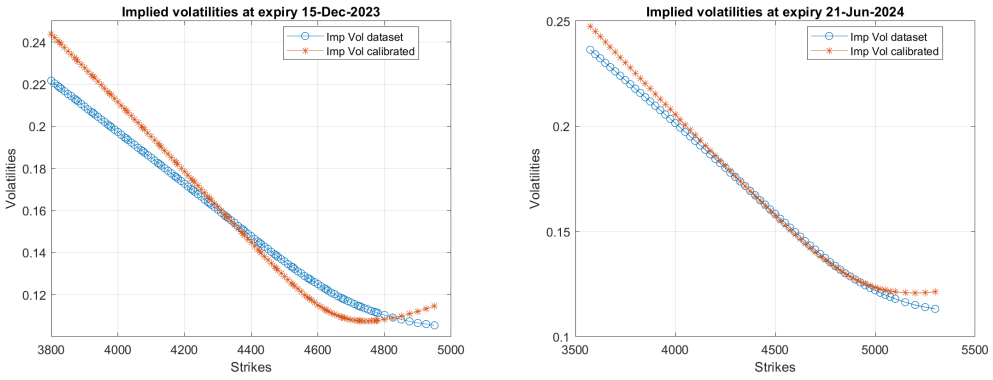

(5a) (5b)

Figure 5: Implied volatilities from market quoted prices (blue lines) and from Levy model prices (orange lines) for options in the American market with expiry 15-Dec-2023 (5a) and 21-Jun-2024 (5b).

European market:

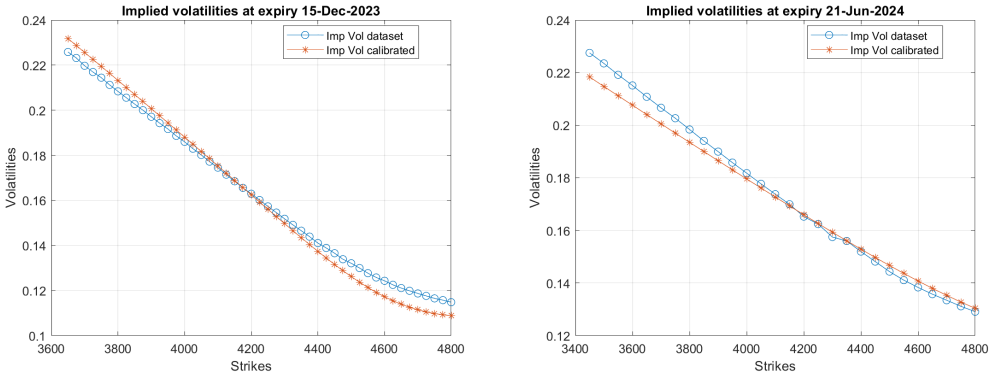

(6a) (6b)

Figure 6: Implied volatilities from market quoted prices (blue lines) and from Levy model prices (orange lines) for options in the European market with expiry 15-Dec-2023 (6a) and 21-Jun-2024 (6b).

We can observe that the model implied volatilities mimic well the market ones. This trend is more present for longer expiries, meanwhile the nearest ones are not always perfectly fitted: in particular, we can highlight that the higher strikes owns a more marked convexity, as can be observed in figure Figure (5a).

To understand better the performance of our calibration, we decide to plot the call and put prices obtained with our calibrated parameters:

American market:

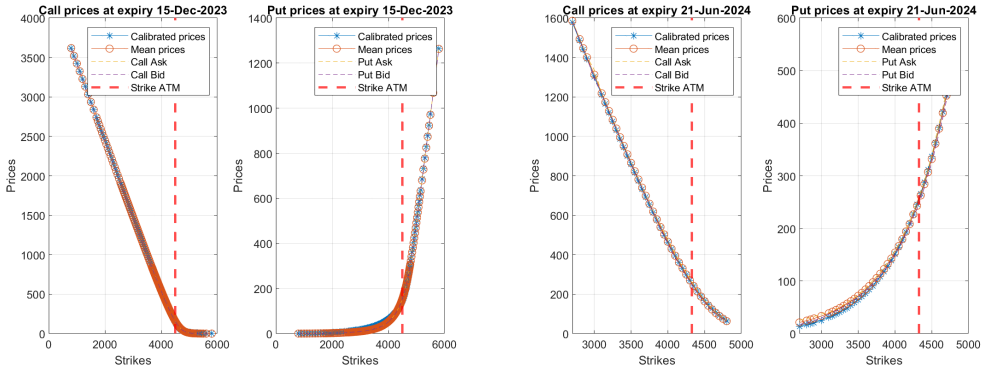

(7a) (7b)

Figure 7: Quoted prices against the corresponding prices obtained via the Levy model for Put and Call options in the American market with expiry 15-Dec-2023 (7a) and 21-Jun-2024 (7b).

European market:

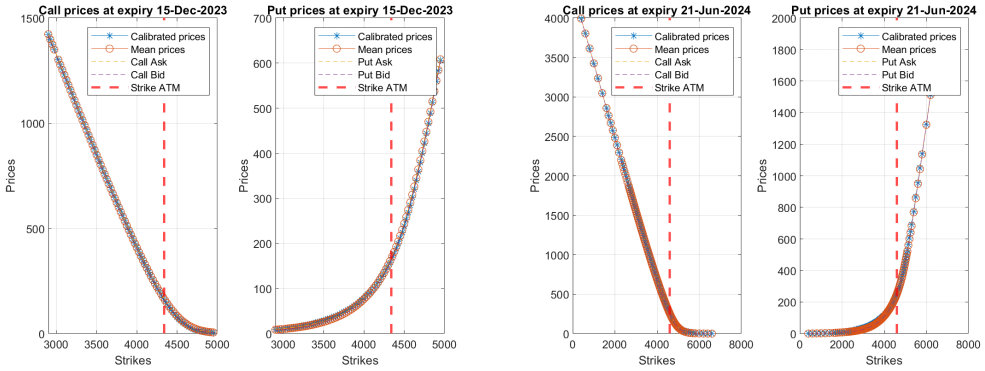

(8a) (8b)

Figure 8: Quoted prices against the corresponding prices obtained via the Levy model for Put and Call options in the European market with expiry 15-Dec-2023 (8a) and 21-Jun-2024 (8b).

From these plots we can observe that the model prices follow closely the market ones.

To have a more quantitative and comprehensive view of how well our parameters performed, we also compute a customized error measure for the model prices, which increments whenever the model price does not fall inside the bid-ask interval. We are mainly interested in the error over the call prices, since the put prices are obtained via the put/call parity and this formula could introduce a further error term due to the fact that the discounts $\bar{B}(0,t)$ are obtained through the least squares formula.

$$\mathscr{E}_{Call}(t_j) = 100 \cdot \sum_K \left[\frac{C_{tj}^{MDL} - C_{tj}^{MKT\,ASK}}{C_{tj}^{MKT\,ASK}} \cdot \mathbb{I}_{C_{tj}^{MDL} > C_{tj}^{MKT\,ASK}} + \frac{C_{tj}^{MKT\,BID} - C_{tj}^{MDL}}{C_{tj}^{MKT\,BID}} \cdot \mathbb{I}_{C_{tj}^{MDL} < C_{tj}^{MKT\,BID}} \right]$$

We compute the mean over the expiries of the errors found, to have a unique error measurement for each market. The results are reported in Table 6. Since the error percentage obtained is significantly low, we can infer that our model reproduces well the market prices.

	Error Call
American market	13.363219 %
European market	2.806288 %

Table 6: Customized error call

7 Correlation comparison: Model vs Historical

The correlation coefficients can be obtained from two different sources: estimating the model correlation from the parameters calibrated or computing the historical correlation over the returns. The result obtained from the two methods are quite different:

	Historical	Calibrated	Nominal Error	% Error
Rho	0.801	0.2911	0.5098	63%

Table 7: Correlation coefficients

The results are quite different even if both represent the same markets. We were able to get a calibrated correlation of the same order of the historical one but the overall parameters were highly inefficient and not theoretically sustainable; therefore, the key assumption that we make is to relax the calibration hypothesis over the rho: we decide to sacrifice precision in the computation of the model correlation in order to obtain parameters that are capable to price correctly the contract and yield good results for volatility's and put-call prices.

In other words we believe that, in our framework which considers the use of NIG processes, the calibrated model cannot obtain a correlation of the same magnitude as the historical one. Calibrating the model was like balancing a tightrope walker: the *fmincon* function in Matlab does not guarantee a global minimum. Therefore adjusting the initial conditions, FFT parameters, and boundaries for minimization can lead to significantly different results.

Parameters are strictly interconnected and they are the result of a multi expiry calibration procedure that cannot precisely describe all the possible markets and maturities:

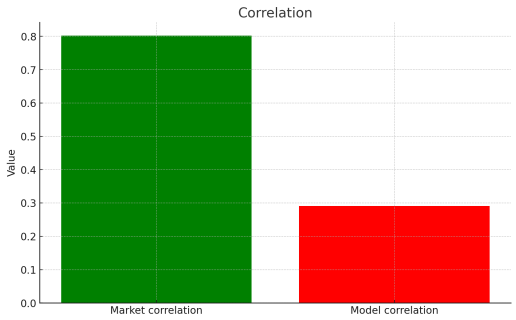

Figure 9: Maximum historical correlation and maximum Levy model correlation with the calibrated parameters.

8 Calibration of the Black model

The computation of the multivariate Levy model should be compare to a more stable and theoretically proved method; therefore we consider a plain Black model which describes the evolution of the prices of the S&P500 and EUROSTOXX50 indices as:

$$X_i(t) = -\frac{1}{2}\sigma_i^2 t + \sigma_i W_i(t) \text{ for } i = 1, 2 \tag{28}$$

where $W_1(t)$ and $W_2(t)$ are two Brownian Motions - $W_i(t) \sim \mathcal{N}(0,t)$ for $i = 1,2$
where $Corr(W_1(t), W_2(T)) = \rho$

The Black model should be calibrated as the previous Levy and the matching of the historical market correlation ρ^{hist} should be discussed deeply.

The model parameters to be calibrated are only the σ_i in order to match the model prices of European Plain Vanilla Options on the S&P500 and EURO STOXX 50 indices.

8.1 Maximum correlation in the Black model framework

Given the correlation among the two Brownian Motions $Corr(W_1(t), W_2(t)) = \rho$, it is possible to show that this correlation holds also among the forward exponents $X_1(t)$ and $X_2(t)$.

Indeed, we can write the correlation between the forward exponents as:

$$Corr(X_1(t), X_2(t)) = \frac{COV(X_1(t), X_2(t))}{\sqrt{Var(X_1(t)) \cdot Var(X_2(t))}} \tag{29}$$

We start by the computation of $Var(X_i(t))$ for $i = 1, 2$:

$$\begin{aligned}
Var(X_i(t)) &= \mathbb{E}[X_i(t)^2] - \mathbb{E}[X_i(t)]^2 = \mathbb{E}\left[\left(-\frac{1}{2}\sigma_i^2 t + \sigma_i W_i(t)\right)^2\right] - \mathbb{E}\left[-\frac{1}{2}\sigma_i^2 t + \sigma_i W_i(t)\right]^2 = \\
&= \mathbb{E}\left[\frac{1}{4}\cdot\sigma_i^4\cdot t^2 - \sigma_i^3\cdot t\cdot W_i(t) + \sigma_i^2\cdot W_i(t)^2\right] - \mathbb{E}\left[-\frac{1}{2}\sigma_i^2 t + \sigma_i W_i(t)\right]^2 = \\
&= \left\{for\ the\ linearity\ of\ the\ expected\ value\ and\ since\ \mathbb{E}[W_i(t)] = 0\right\} = \\
&= \frac{1}{4}\cdot\sigma_i^4\cdot t^2 + \sigma_i^2\cdot\mathbb{E}\big[W_i(t)^2\big] - \frac{1}{4}\cdot\sigma_i^4\cdot t^2 = \sigma_i^2\cdot\mathbb{E}\big[W_i(t)^2\big] = \\
&= \left\{from\ the\ definition\ of\ variance\right\} = \\
&= \sigma_i^2\cdot\big(Var(W_i(t)) + \mathbb{E}\big[W_i(t)\big]^2\big) = \\
&= \left\{since\ Var(W_i(t)) = t\ and\ \mathbb{E}\big[W_i(t)\big] = 0\right\} = \sigma_i^2\cdot t
\end{aligned} \tag{30}$$

To compute the covariance between $X_1(t)$ and $X_2(t)$, we start by computing the local covariance, making the assumption that the correlation of two infinitesimal variations of the two Brownian Motion results is equal to the correlation ρ times dt (i.e. $Corr(dW_1(t), dW_2(t)) = \mathbb{E}\big[dW_1(t)\cdot dW_2(t)\big] - \mathbb{E}\big[dW_1(t)\big]\cdot\mathbb{E}\big[dW_2(t)\big] = \rho dt$).

Thanks to this assumption, the following computations hold:

$$\begin{aligned}
&COV(dX_1(t), dX_2(t)) = \mathbb{E}\big[dX_1(t)\cdot dX_2(t)\big] - \mathbb{E}\big[dX_1(t)\big]\cdot\mathbb{E}\big[dX_2(t)\big] = \\
&= \mathbb{E}\left[\left(-\frac{1}{2}\sigma_1^2 dt + \sigma_1 dW_1(t)\right)\cdot\left(-\frac{1}{2}\sigma_2^2 dt + \sigma_2 dW_2(t)\right)\right] + \\
&\quad - \mathbb{E}\left[-\frac{1}{2}\sigma_1^2 dt + \sigma_1 dW_1(t)\right]\cdot\mathbb{E}\left[-\frac{1}{2}\sigma_2^2 dt + \sigma_2 dW_2(t)\right] = \\
&= \frac{1}{4}\sigma_1^2\sigma_2^2 dt\cdot dt + \sigma_1\sigma_2\mathbb{E}\big[dW_1(t)\cdot dW_2(t)\big] - \frac{1}{2}\sigma_1^2\sigma_2 dt\mathbb{E}\big[dW_2(t)\big] - \frac{1}{2}\sigma_2^2\sigma_1 dt\mathbb{E}\big[dW_1(t)\big] - \frac{1}{4}\sigma_1^2\sigma_2^2 dt\cdot dt = \\
&= \left\{by\ simplifying\ the\ opposite\ terms\ and\ since\ \mathbb{E}[dW_i(t)] = 0\ for\ i = 1,2\right\} = \\
&= \sigma_1\sigma_2\mathbb{E}\big[dW_1(t)\cdot dW_2(t)\big] = \\
&= \left\{thanks\ to\ the\ assumption\ and\ to\ the\ fact\ that\ \mathbb{E}[dW_i(t)] = 0\ for\ i = 1,2\right\} = \\
&= \sigma_1\sigma_2\rho dt
\end{aligned}$$

Integrating this result between 0 and t, we get:

$$COV(X_1(t), X_2(t)) = \int_0^t \sigma_1 \sigma_2 \rho dt = \sigma_1 \sigma_2 \rho t \tag{31}$$

By substitution of (30) and (31) in the expression (29), we can finally retrieve the correlation value:

$$Corr(X_1(t), X_2(t)) = \frac{\sigma_1 \cdot \sigma_2 \cdot \rho \cdot t}{\sqrt{\sigma_1^2 \cdot t \cdot \sigma_2^2 \cdot t}} = \frac{\sigma_1 \cdot \sigma_2 \cdot \rho \cdot t}{\sigma_1 \cdot \sigma_2 \cdot t} = \rho \tag{32}$$

From this result, we can conclude that in the Black model the maximum value of correlation attainable is $\rho = 1$, while the minimum is $\rho = -1$, since there are no constraints about the correlation of two Brownian Motions.

Moreover, when this model is applied to describe the evolution of the S&P500 and EUROSTOXX50 indices, it will be possible to exactly match the historical correlation ρ^{hist} mentioned before. This is a first big difference from the multivariate Levy model.

However, even if the Black model seems to match better the historical correlation, we expect it to have a worse performance in terms of pricing precision with respect to the multivariate Levy model, since a unique parameter for the volatility is used to price options with different strikes and maturities.

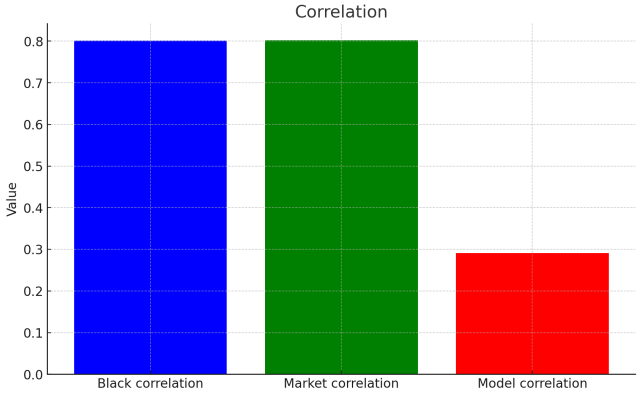

Figure 10: Maximum Black model correlation, and maximum Levy model correlation with the calibrated parameters.

8.2 Black model calibration

The calibration of the Black model should be done minimizing the least square error between the model prices and the quoted prices. Similarly to what it was done for the Levy calibration, only the OTM options with $|\Delta_{Black\&Scholes}| \in [10\%, 90\%]$ were kept in the calibration dataset, and we use the same expiries selected in the Levy calibration (see **Appendix 3**) to have more comparable results.

In this case, it is needed to calibrate separately among the two implied volatility surfaces: there is not any possibility to keep track of the correlation when we try to calibrate the volatilities σ_i, however it is always possible to take into account it when the dynamics is simulated via a Monte-Carlo.

The objective function to minimize is:

$$\Pi_i = \underset{\sigma_i \ i=1,2}{\arg\min} \sum_{t=1}^{T} \left[\sum_{j:K_j<F_t} \left(P_{tj}^{MKT} - P_{tj}^{MODEL}(\sigma_i) \right)^2 + \sum_{j:K_j>F_t} \left(C_{tj}^{MKT} - C_{tj}^{MODEL}(\sigma_i) \right)^2 \right] \tag{33}$$

where T is the total number of maturities

where C_{tj}^{MKT} and P_{tj}^{MKT} are the Call and Put market prices

where $C_{tj}^{MODEL}(\sigma_i)$ and $P_{tj}^{MODEL}(\sigma_i)$ are the model prices

The call options are obtained via the Black formula, using the discounts $\bar{B}(0,t)$ and the forward prices $F(0,t)$ found in Section 5, while put options are computed via the Put-Call parity, using the same expression introduced in equation (26). The only constraint imposed is the positivity of the two volatilities.

The calibrated values of the two volatilities are reported the following table.

σ_{USA}	σ_{EU}
0.1603	0.1569

Table 8: Calibrated volatilities for the Black model.

We observe that also the Black model reflects the higher volatility of the American market, even if the two calibrated values differ by just 34bps. In addition, these volatilities are higher than the marginal mean value voltilities obtained for the Levy model.

8.3 Analysis of the calibrated Black model

To have a graphical visualization of the obtained results, we plot the model put and call prices obtained using the calibrated Black volatilities against the market prices. In order to make these results comparable with the Levy model results, we report the graphs obtained for the same expiries chosen above for both the American and the European market.

American market:

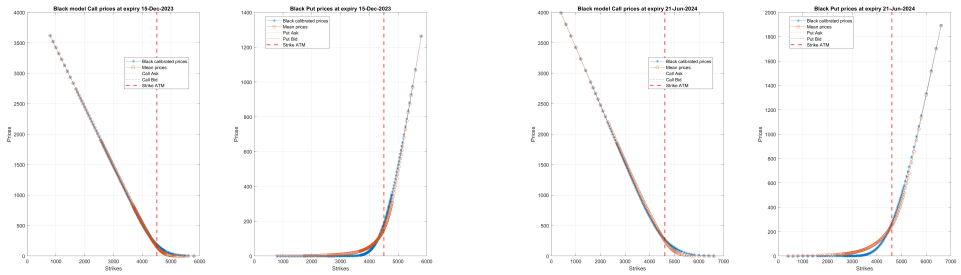

(11a) (11b)

Figure 11: Quoted prices against the corresponding prices obtained via the Black model for Put and Call options in the American market with expiry 15-Dec-2023 (11a) and 21-Jun-2024 (11b).

European market:

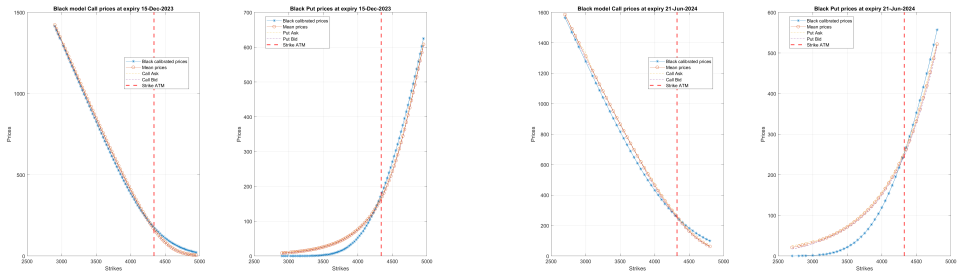

(12a) (12b)

Figure 12: Quoted prices against the corresponding prices obtained via the Black model for Put and Call options in the European market with expiry 15-Dec-2023 (12a) and 21-Jun-2024 (12b).

Comparing these graphs with the Levy model prices' plots (see Figure 7 and Figure 8), we can immediately notice that the Black model seems to have a greater error on the prices, especially for the European market Put options. From theoretical point of view, this result is not surprising, since the Black model has a significant simplification and reduction of parameters, e.g. we consider a unique volatility value for all strikes and expiries.

In order to have a more quantitative comparison, we can also compute the mean percentage error in the prices: the results are reported in Table 9 and they confirm the qualitative observations.

	Error Call
American market	47.177447 %
European market	22.167362 %

Table 9: Customized error call

9 Pricing of the exotic option

In this section, the Levy and the Black model calibrated above are used to price a derivative with payoff:

$$(S_1(T) - S_1(0))^+ \cdot \mathbb{I}_{S_2(T)<0.95\cdot S_2(0)} \tag{34}$$

where, congruently to the notation used in this report, $S_1(t)$ and $S_2(t)$ are the spot prices of the S&P500 and EUROSTOXX50 respectively and the maturity T is equal to one year.

In order to price this contract we need to make an assumption on the one year discount factor: this structured product depends on both the American and the European market, therefore we need to decide which discount factor we are going to use. It can be noticed that the linear part of the payoff only depends on the spot price of the S&P500, therefore we decide to discount the payoff using the $\bar{B}_{USA}(0,T)$ of the American market.

This value of the discount is not among the discounts computed in Section 5.3, thus we need to find a way to interpolate it. We make another assumption by stating that form the discounts obtained via the synthetic forwards, it is possible to retrieve a market zero rate $r_{market,i}$ for $i = 1, 2$ which is able to take into account both the interest rates and the eventual dividends. This rate can be computed as:

$$r_{market,i}(t) = -\frac{ln(\bar{B}_i(0,t))}{t} \tag{35}$$

We interpolate the rates found via this formula in order to find $r_{market,1}(T)$, the one-year American market zero-rate. From this, it is possible to compute the one-year discount of the American market as:

$$\bar{B}_1(0,T) = e^{-r_{market,1}(T)\cdot T} \tag{36}$$

This is the value of the discount that we are going to use in the following sections.

The last consideration regards the initial forward price that will be used in the forwards simulations via the two models. Again, since we do not have the one-year forward prices among the forwards computed in Section 5.3, we need to find a way to retrieve this value. A possible solution is to assume that to pass from the available spot prices of the indexes of the two markets to the corresponding forwards, we can use the Garman-Kohlhagen formula, considering the interpolated market rate $r_{market,i}(t)$. Therefore, the following relationship must hold:

$$F_i(0,T) = S_i(0) \cdot e^{r_{market,i}(T)\cdot T} \tag{37}$$

9.1 Pricing with Levy

The Levy model calibrated in Section 6 can be used to price the derivative contract. To determine the payoff in T, it is needed to know the value of the two spots in T, which can be computed by simulating the forwards, remembering that $F_i(T,T) = S_i(T)$.

We recall that the dynamics of the forward in this model can be described as:

$$F_i(t,t) = F_i(0,t) \cdot e^{X_i(t)+p_i \cdot t} = F_i(0,t) \cdot e^{Y_i(t)+a_i \cdot Z(t)+p_i \cdot t} \qquad \text{for } i = 1,2 \tag{38}$$

To maintain the correlation structure between the forward prices of the S&P500 and the EUROSTOXX50 indexes, it is important to simulate the two different idiosyncratic factors $Y_i(t)$ and a common systematic factor $Z(t)$.

Given the three NIG processes $Y_1(t) \sim NIG(\nu_1, \beta_1, \gamma_1)$, $Y_2(t) \sim NIG(\nu_2, \beta_2, \gamma_2)$ and $Z(t) \sim NIG(\nu_Z, \beta_Z, \gamma_Z)$ with the previously calibrated parameters, we simulate their dynamics thanks to the following equivalent-in-law formulation:

$$Y_i(t) = \sqrt{t} \cdot \gamma_i \cdot \sqrt{G_i} \cdot g_i + \beta_i \cdot t \cdot G_i \text{ for } i = 1,2 \qquad Z(t) = \sqrt{t} \cdot \gamma_Z \cdot \sqrt{G_Z} \cdot g_Z + \beta_Z \cdot t \cdot G_Z$$

$$\text{where } G_j \sim IG\left(1, \frac{\nu_j}{t}\right) \text{ and } g_j \sim \mathcal{N}(0,1) \text{ for } j = 1,2,Z$$

The simulated values, together with the initial forward values $F_i(0,T)$ and the drift compensators p_i, were substituted in the expression reported in (38) to obtain $F_i(T,T) = S_i(T)$.

The price of the derivative was finally computed evaluating the payoff with the simulated values, finding the mean value and discounting it with $\bar{B}_1(0,T)$. The result is reported in Table 10.

9.2 Levy model semi-closed formula

Finding a closed formula for the Levy model is notably difficult, since a double integral in the correlated NIG random variables $X_1(t)$ and $X_2(t)$ needs to be solved, or a triple integral in $Y_1(t)$, $Y_2(t)$, and $Z(t)$ must be computed. However, it is still possible to retrieve a semi-closed formula exploiting the numerical integration of MATLAB.

From the dynamics of the forwards described in (38), and by assuming that from the market discounts $\bar{B}(0,t)$ we can retrieve a market rate $r_{market,i} = r_i$ which considers both the interest rate and the eventual presence of dividends, we can describe the spot dynamics of the two indices thanks to the Garman-Kohlhagen formula as:

$$S_i(t) = S_i(0) \cdot exp\left\{ r_i \cdot t + Y_i(t) + a_i \cdot Z(t) + p_i \cdot t \right\} \text{ for } i = 1,2$$

The main idea falls on the conditioning of the Processes Y_1 and Y_2 with respect to the systematic part $Z(t)$, exploiting a property of the conditional random vectors and the independence of Y_1 and Y_2:

$$f_{((Y_1,Y_2),Z)}(y_1,y_2,z) = f_{(Y_1,Y_2)|Z}(y_1,y_2) \cdot f_Z(z) = f_{Y_1|Z}(y_1) \cdot f_{Y_2|Z}(y_2) \cdot f_Z(z)$$

All the previous process theoretical assumptions are still maintained:

$$\mathbb{E}_0\Big[D(0,t)\cdot(S_1(t)-S_1(0))^+\cdot\mathbb{I}_{S_2(t)\leq 0.95\cdot S_2(0)}\Big]=$$
$$=B(0,t)\cdot\int_{-\infty}^{\infty}(S_1(0)\cdot e^{r_1\cdot t+Y_1(t)+a_1\cdot Z(t)+p_1\cdot t}-S_1(0))^+\cdot$$
$$\cdot\,\mathbb{I}_{S_2(0)\cdot e^{r_2\cdot t+Y_2(t)+a_2\cdot Z(t)+p_2\cdot t}\leq 0.95\cdot S_2(0)}\cdot f_{(Y1,Y2,Z)}\cdot dy_1\cdot dy_2\cdot dZ=$$

$$=\big\{\textit{simplifying the notation and grouping together the similar terms}\big\}=$$

$$=B(0,t)\cdot\int_{-\infty}^{\infty}\int_{-\infty}^{\infty}(S_1(0)\cdot(e^{r_1\cdot t+Y_1(t)+a_1\cdot Z(t)+p_1\cdot t}-1))^+\cdot\mathbb{I}_{(\dots)\leq 0.95}\cdot f_{(Y1,Y2\ |\ Z=z)}\cdot dy_1\cdot dy_2\cdot f(dZ)=$$
$$=S_1(0)\cdot B(0,t)\cdot\int_{-\infty}^{\infty}\int_{-\infty}^{\infty}(e^{r_1\cdot t+Y_1(t)+a_1\cdot Z(t)+p_1\cdot t}-1)^+\cdot\mathbb{I}_{(\dots)\leq 0.95}\cdot f_{(Y1,Y2\ |\ Z=z)}\cdot dy_1\cdot dy_2\cdot f(dZ)=$$
$$=S_1(0)\cdot B(0,t)\cdot\int_{-\infty}^{\infty}\mathbb{E}_0\big[(e^{r_1\cdot t+Y_1(t)+a_1\cdot Z(t)+p_1\cdot t}-1)^+\cdot\mathbb{I}_{(\dots)\leq 0.95}|Z=z\big]\cdot f(dZ)=$$

$$=\big\{\textit{recalling that the idiosyncratic parts are independent from each other}\big\}=$$

$$=S_1(0)\cdot B(0,t)\cdot\int_{-\infty}^{\infty}\mathbb{E}_0\big[(e^{r_1\cdot t+Y_1(t)+a_1\cdot Z(t)+p_1\cdot t}-1)^+|Z=z\big]\cdot\mathbb{E}_0\big[\mathbb{I}_{(\dots)\leq 0.95}|Z=z\big]\cdot f(dZ)=$$
$$=S_1(0)\cdot B(0,t)\cdot\int_{-\infty}^{\infty}(A)\cdot(B)\cdot f(dZ)$$

Let's now focus on the different parts separately in order to solve them:

$$(B)=\mathbb{E}_0\big[\mathbb{I}_{e^{r_2\cdot t+Y_2(t)+a_2\cdot Z(t)+p_2\cdot t}\leq 0.95}|Z=z\big]=\mathbb{E}_0\big[\mathbb{I}_{Y_2(t)\leq ln(0.95)-r_2\cdot t-a_2\cdot Z(t)-p_2\cdot t}|Z=z\big]=$$
$$=\mathbb{P}(Y_2(t)\leq ln(0.95)-r_2\cdot t-a_2\cdot Z(t)-p_2\cdot t)=$$

$$=\big\{\textit{taking the short notation } d_3=ln(0.95)-r_2\cdot t-a_2\cdot Z(t)-p_2\cdot t\big\}=$$

$$=\mathrm{NIG}(d_3)$$

$$(A)=\mathbb{E}_0\big[(e^{r_1\cdot t+Y_1(t)+a_1\cdot Z+p_1\cdot t}-1)^+|Z=z\big]=$$
$$=\mathbb{E}_0\big[e^{r_1\cdot t+Y_1(t)+a_1\cdot Z+p_1\cdot t}\cdot\mathbb{I}_{e^{r_1\cdot t+Y_1(t)+a_1\cdot Z+p_1\cdot t}>1}-\mathbb{I}_{e^{r_1\cdot t+Y_1(t)+a_1\cdot Z+p_1\cdot t}>1}|Z=z\big]=$$
$$=\mathbb{E}_0\big[e^{r_1\cdot t+Y_1(t)+a_1\cdot Z+p_1\cdot t}\cdot\mathbb{I}_{e^{r_1\cdot t+Y_1(t)+a_1\cdot Z+p_1\cdot t}>1}\big]-\mathbb{E}_0\big[\mathbb{I}_{e^{r_1\cdot t+Y_1(t)+a_1\cdot Z+p_1\cdot t}>1}|Z=z\big]=$$
$$=(C)-(D)$$

Let's compute again the sub-cases of the previous equations:

$$(C)=\mathbb{E}_0\big[e^{r_1\cdot t+Y_1(t)+a_1\cdot Z+p_1\cdot t}\cdot\mathbb{I}_{e^{r_1\cdot t+Y_1(t)+a_1\cdot Z+p_1\cdot t}>1}\big]=$$
$$=e^{r_1\cdot t+a_1\cdot Z+p_1\cdot t}\cdot\mathbb{E}_0\big[e^{Y_1(t)}\cdot\mathbb{I}_{Y_1(t)>-r_1\cdot t-a_1\cdot Z-p_1\cdot t}\big]=$$
$$=e^{r_1\cdot t+a_1\cdot Z+p_1\cdot t}\cdot\int_{-\infty}^{\infty}e^{Y_1(t)}\cdot\mathbb{I}_{Y_1(t)>-r_1\cdot t-a_1\cdot Z-p_1\cdot t}\cdot dy_1=$$

$$=\big\{\textit{taking the short notation } d_1=-r_1\cdot t-a_1\cdot Z-p_1\cdot t\big\}=$$

$$=e^{r_1\cdot t+a_1\cdot Z+p_1\cdot t}\cdot\int_{d_1}^{\infty}e^{Y_1(t)}\cdot\mathbb{I}_{Y_1(t)>d_1}\cdot dy_1$$

$$(D) = \mathbb{E}_0\left[\mathbb{I}_{e^{r_1\cdot t+Y_1(t)+a_1\cdot Z+p_1\cdot t}>1}|Z=z\right] =$$

$$= \{\textit{considering the cumulative distribution function of the NIG process as described in (B)}\} =$$
$$= \{\textit{taking the short notation } d_2 = -r_1\cdot t - a_1\cdot Z - p_1\cdot t\} =$$

$$= 1 - NIG(d_2)$$

Therefore putting everything together, we can obtain that:

$$Price = S_1(0)\cdot B(0,t)\cdot\int_{-\infty}^{\infty}\left(e^{r_1\cdot t+a_1\cdot Z+p_1\cdot t}\cdot\int_{d_1}^{\infty}e^{Y_1(t)}\cdot\mathbb{I}_{Y_1(t)>d_1}\cdot dy_1 - (1-NIG(d_2))\right)\cdot \text{NIG}(d_3)\cdot f(dZ)$$

The cumulative NIG distribution are computed numerically integrating the density function as described in the Cont & Tankov book and following reported:

$$p_t(x) = G\cdot e^{E\cdot x}\cdot\frac{K_1(F\cdot\sqrt{x^2+\frac{t^2\cdot\sigma^2}{\kappa}})}{\sqrt{x^2+\frac{t^2\cdot\sigma^2}{\kappa}}}$$

where $E = \dfrac{\theta}{\sigma^2}$ $\quad F = \sqrt{\theta^2+\dfrac{\sigma^2}{\kappa}}$ $\quad G = \dfrac{t}{\pi}\cdot e^{\frac{t}{\kappa}}\cdot\sqrt{\dfrac{\theta^2}{\kappa\cdot\sigma^2}+\dfrac{1}{\kappa^2}}$

where $K_1()$ is the Bessel function of the second kind

9.3 Pricing with Black

In order to price the product via the Black model, we consider the equality in law of the dynamics of the forward prices of the S&P500 and the EUROSTOXX50:

$$F_i(t) = F_{0,i}\cdot exp\left\{-\frac{1}{2}\sigma_i^2 t+\sigma_i W_i(t)\right\}\overset{\text{law}}{=}F_{0,i}\cdot exp\left\{-\frac{1}{2}\sigma_i^2 t+\sigma_i\sqrt{t}g_i\right\}\text{ for } i=1,2$$

$$\text{where } g_i\sim\mathcal{N}(0,1)$$

To simulate the forwards, we make the following considerations:

- We use the calibrated values of the Black volatilities σ_i reported in Table 8.
- To keep track of the correlation among the two Brownian Motions, we simulate a multivariate Gaussian vector (g_1, g_2) with zero mean and covariance matrix

$$\Sigma = \begin{bmatrix}1 & \rho\\ \rho & 1\end{bmatrix}$$

  In order to reduce the variance of the simulated forward values, in the Monte-Carlo simulation it is used also the antithetic variables technique.

- The initial forward price $F_{0,i} = F_i(0,t)$ is obtained via the expression in (37).
- The mean payoff that we obtain is discounted using the one-year American discount factor $\bar{B}_1(0,T)$.

The derivative's price obtained and the corresponding 95% confidence interval are reported in Table 10.

9.4 Black model semi-closed formula

To price the product with a closed formula in the Black model framework, we consider the dynamics of the forward prices of the S&P500 and the EURO STOXX 50 described by the following expression:

$$F_i(t) = F_{0,i} \cdot exp\Big\{ -\frac{1}{2}\sigma_i^2 t + \sigma_i W_i(t) \Big\} \text{ for } i = 1, 2$$

As states above, we assume that from the market discounts $\bar{B}(0,t)$ found in Section (3) we can retrieve a rate $r_{market,i} = r_i$, which takes into account the interest rate and the eventual dividends (if any); therefore, we can describe the spot dynamics of the two indices thanks to the Garman-Kohlhagen formula as:

$$S_i(t) = S_0 \cdot exp\Big\{ \Big(r_i - \frac{1}{2}\sigma_i^2 \Big) t + \sigma_i W_i(t) \Big\} \text{ for } i = 1, 2$$

Where the joint probability distribution of the two Brownian Motions $W_1(t)$ and $W_2(t)$ is given by

$$\big(W_1(t), W_2(t)\big) \sim \mathcal{N}\left(\begin{bmatrix} 0 \\ 0 \end{bmatrix}, \begin{bmatrix} t & \rho t \\ \rho t & t \end{bmatrix} \right)$$

First of all, we state that finding a closed formula for this particular payoff is not an easy task, since a double integral in the two Brownian Motions W_1 and W_2 needs to be solved. To simplify this computation and to retrieve a price comparable with the price obtained via the Monte-Carlo simulation, it is possible to find a solution via a semi-closed formula.

The main idea behind the computations that will be reported below is to pass from the joint distribution of W_1 and W_2 to the conditional probability distribution times the marginal probability, using the properties of the conditional probability:

$$f_{W_1,W_2}(w_1, w_2) = f_{W_1|W_2}(w_1) \cdot f_{W_2}(w_2) \tag{39}$$

The second step to complete the computation is to find a way to write the conditional probability. In order to resolve this there are two possible approaches: the firs one uses a property of Brownian Motions, while the second one exploits the properties of conditioned Gaussian Vectors.

We start by presenting the first possible approach, whose key idea is to write the Brownian Motions W_1 in terms of W_2, using a property of the correlated Brownian Motions, as expressed in the following proposition.

Proposition 9.1:
Given two Brownian Motions $W_1(t)$ and $W_2(t)$ such that $Corr(W_1(t), W_2(t)) = \rho$, we can write

$$W_1(t) = \rho W_2(t) + \sqrt{1-\rho^2} B_1(t) \tag{40}$$

where $B_1(t)$ is a Brownian Motion such that $B_1(t) \sim \mathcal{N}(0,t)$ and $B_1(t) \perp W_2(t)$.

Proof:
We need to prove that $W_1(t)$ defined as in (40) is still a Brownian Motion and that it keeps the same correlation with $W_2(t)$.

To prove that $W_1(t)$ is a Brownian Motion we use an equivalent definition:

- $W_1(0) \overset{\text{a.s.}}{=} 0$, indeed $W_1(0) = \rho W_2(0) + \sqrt{1-\rho^2} B_1(0) \overset{\text{a.s.}}{=} 0$, since $W_2(t)$ and $B_1(t)$ are two Brownian Motions.
- We prove that for $0 \le t_1 \le t_2 \le ... \le t_n$, $(W_1(t_1), ..., W_1(t_n)) \sim \mathcal{N}(0, \Gamma)$.

  This can be directly proved by observing that:

$$(W_1(t_1), ..., W_1(t_n)) = \begin{bmatrix} \rho W_2(t_1) + \sqrt{1-\rho^2} B_1(t_1) \\ \vdots \\ \rho W_2(t_n) + \sqrt{1-\rho^2} B_1(t_n) \end{bmatrix} = \rho \begin{bmatrix} W_2(t_1) \\ \vdots \\ W_2(t_n) \end{bmatrix} + \sqrt{1-\rho^2} \begin{bmatrix} B_1(t_1) \\ \vdots \\ B_1(t_n) \end{bmatrix}$$

$(W_1(t_1), ..., W_1(t_n))$ is Gaussian vector since it is the linear combination of two independent Gaussian vectors.
To prove that the mean vector is a vector of zeros it is sufficient to observe that for every t:

$$\begin{aligned}\mathbb{E}[W_1(t))] &= \mathbb{E}[\rho W_2(t) + \sqrt{1-\rho^2}B_1(t)] = \\ &= \rho\ \mathbb{E}[W_2(t)] + \sqrt{1-\rho^2}\ \mathbb{E}[B_1(t)] = \\ &= 0\end{aligned}$$

where we used the linearity of the expected value and the laws of $W_2(t)$ and $B_1(t)$.

- Finally, for every $s,\ t$ we have that $\mathbb{E}[W_1(t)\ W_1(s)] = \min(s,t)$, indeed:

$$\begin{aligned}\mathbb{E}[W_1(t)\ W_1(s)] &= \mathbb{E}[(\rho W_2(t) + \sqrt{1-\rho^2}B_1(t))(\rho W_2(s) + \sqrt{1-\rho^2}B_1(s))] = \\ &= \rho^2\mathbb{E}[W_2(t)W_2(s)] + \rho\sqrt{1-\rho^2}\mathbb{E}[W_2(t)B_1(s)] + \rho\sqrt{1-\rho^2}\mathbb{E}[W_2(s)B_1(t)] + \\ &\quad + (1-\rho^2)\mathbb{E}[B_1(t)B_1(s)] = \\ &= \rho^2 \cdot \min(s,t) + (1-\rho^2)\cdot\min(s,t) = \\ &= \min(s,t)\end{aligned}$$

Form these three conditions, we can deduce that $W_1(t)$ is a Brownian Motion with respect to the natural filtration.

It remains to prove that $Corr(W_1(t), W_2(t)) = \rho$:

$$Corr(W_1(t), W_2(t)) = \frac{\mathbb{E}[W_1(t)\ W_2(t)] - \mathbb{E}[W_1(t)]\cdot\mathbb{E}[W_2(t)]}{\sqrt{Var(W_1(t))\cdot Var(W_2(t))}}$$

We already know that $\mathbb{E}[W_1(t)] = \mathbb{E}[W_2(t)] = 0$ and $Var(W_1(t)) = t$.
We observe that:

$$\begin{aligned}Var(W_1(t)) &= \mathbb{E}[W_1(t)^2] - \mathbb{E}[W_1(t)]^2 = \mathbb{E}[W_1(t)\cdot W_1(t)] \\ &= \{\textit{using the covariance function of } W_1 \textit{ retireved above}\} = \\ &= t\end{aligned}$$

while, to determine the covariance between W_1 and W_2, we can immediately compute:

$$\begin{aligned}\mathbb{E}[W_1(t)\ W_2(t)] &= \mathbb{E}[(\rho W_2(t) + \sqrt{1-\rho^2}B_1(t))\cdot\ W_2(t)] = \\ &= \rho\mathbb{E}[W_2(t)^2] + \sqrt{1-\rho^2}\mathbb{E}[B_1(t)\cdot\ W_2(t)] = \\ &= \rho t\end{aligned}$$

Therefore, we can conclude the proof by observing that:

$$Corr(W_1(t), W_2(t)) = \frac{\mathbb{E}[W_1(t)\ W_2(t)] - \mathbb{E}[W_1(t)]\cdot\mathbb{E}[W_2(t)]}{\sqrt{Var(W_1(t))\cdot Var(W_2(t))}} = \frac{\rho t}{\sqrt{t\cdot t}} = \rho$$

□

Using this Proposition, we can start to report the computations to obtain the semi-closed formula: we compute the expected value in $t = 0$ of the payoff.

$$\begin{aligned}
&\mathbb{E}_0\Big[D_1(0,t)\cdot(S_1(t)-S_1(0))^+\cdot\mathbb{I}_{S_2(t)<0.95\cdot S_2(0)}\Big] = \\
&= \big\{\textit{assuming that the discount is deterministic and considering the dynamics of } S_2(t)\big\} = \\
&= \bar{B}_1(0,t)\cdot\mathbb{E}_0\Big[(S_1(t)-S_1(0))^+\cdot\mathbb{I}_{S_2(0)\exp\left\{\left(r_2-\frac{1}{2}\sigma_2^2\right)t+\sigma_2 W_2(t)\right\}<0.95\cdot S_2(0)}\Big] = \\
&= \bar{B}_1(0,t)\cdot\mathbb{E}_0\Big[(S_1(t)-S_1(0))^+\cdot\mathbb{I}_{W_2(t)<\frac{ln(0.95)-(r_2-\frac{1}{2}\sigma_2^2)t}{\sigma_2}}\Big] = \\
&= \bar{B}_1(0,t)\cdot\int_{-\infty}^{\infty}\Big[(S_1(t)-S_1(0))^+\cdot\mathbb{I}_{w_2<\frac{ln(0.95)-(r_2-\frac{1}{2}\sigma_2^2)t}{\sigma_2}}\Big]f_{W_1,W_2}(dw_1,dw_2) = \\
&= \big\{\textit{using equation (39)}\big\} = \\
&= \bar{B}_1(0,t)\cdot\int_{-\infty}^{\infty}\int_{-\infty}^{\infty}\Big[(S_1(t)-S_1(0))^+\cdot\mathbb{I}_{w_2<\frac{ln(0.95)-(r_2-\frac{1}{2}\sigma_2^2)t}{\sigma_2}}\Big]f_{W_1|W_2=w_2}(w_1)dw_1\cdot f_{W_2}(w_2)dw_2 = \\
&= \bar{B}_1(0,t)\cdot\int_{-\infty}^{\infty}\mathbb{E}_0\Big[(S_1(t)-S_1(0))^+\cdot\mathbb{I}_{w_2<\frac{ln(0.95)-(r_2-\frac{1}{2}\sigma_2^2)t}{\sigma_2}}\Big|W_2(t)=w_2\Big]f_{W_2}(dw_2) \\
&= \big\{\textit{since the indicator function is } W_2-\textit{measurable, it can be taken out}\big\} = \\
&= \bar{B}_1(0,t)\cdot\int_{-\infty}^{\infty}\mathbb{E}_0\Big[(S_1(t)-S_1(0))^+\Big|W_2(t)=w_2\Big]\mathbb{I}_{w_2<\frac{ln(0.95)-(r_2-\frac{1}{2}\sigma_2^2)t}{\sigma_2}}f_{W_2}(w_2)dw_2 \qquad (41)
\end{aligned}$$

At this point we focus the attention on the computation of the expectation:

$$\begin{aligned}
&\mathbb{E}_0\Big[(S_1(t)-S_1(0))^+\Big|W_2(t)=w_2\Big] = \\
&= \mathbb{E}_0\Big[(S_1(t)-S_1(0))\cdot\mathbb{I}_{S_1(0)\exp\left\{\left(r_1-\frac{1}{2}\sigma_1^2\right)t+\sigma_1 W_1(t)\right\}>S_1(0)}\Big|W_2(t)=w_2\Big] = \\
&= \big\{\textit{for the linearity of the expected value and since } S_1(0) \textit{ is deterministic}\big\} = \\
&= \mathbb{E}_0\Big[S_1(t)\cdot\mathbb{I}_{W_1(t)>-\frac{\left(r_1-\frac{1}{2}\sigma_1^2\right)t}{\sigma_1}}\Big|W_2(t)=w_2\Big] - S_1(0)\cdot\mathbb{E}_{0,W_1}\Big[\mathbb{I}_{W_1(t)>-\frac{\left(r_1-\frac{1}{2}\sigma_1^2\right)t}{\sigma_1}}\Big|W_2(t)=w_2\Big] \qquad (42)
\end{aligned}$$

We proceed by computing the expectation in the second term:

$$\begin{aligned}
&\mathbb{E}_0\Big[\mathbb{I}_{W_1(t)>-\frac{\left(r_1-\frac{1}{2}\sigma_1^2\right)t}{\sigma_1}}\Big|W_2(t)=w_2\Big] = \big\{\textit{by using Proposition 9.1}\big\} = \\
&= \mathbb{E}_0\Big[\mathbb{I}_{\rho W_2(t)+\sqrt{1-\rho^2}B_1(t)>-\frac{\left(r_1-\frac{1}{2}\sigma_1^2\right)t}{\sigma_1}}\Big|W_2(t)=w_2\Big] = \mathbb{E}_0\Big[\mathbb{I}_{B_1(t)>\frac{-\frac{\left(r_1-\frac{1}{2}\sigma_1^2\right)t}{\sigma_1}-\rho W_2(t)}{\sqrt{1-\rho^2}}}\Big|W_2(t)=w_2\Big] = \\
&= \mathbb{E}_0\Big[\mathbb{I}_{\frac{B_1(t)}{\sqrt{t}}>\frac{-\left(r_1-\frac{1}{2}\sigma_1^2\right)t-\rho w_2\sigma_1}{\sigma_1\cdot\sqrt{t}\cdot\sqrt{1-\rho^2}}}\Big] = \big\{\textit{since } \frac{B_1(t)}{\sqrt{t}}\sim\mathbb{N}(0,1)\big\} = \\
&= 1-\mathcal{N}\left(\frac{-\left(r_1-\frac{1}{2}\sigma_1^2\right)t-\rho w_2\sigma_1}{\sigma_1\cdot\sqrt{t}\cdot\sqrt{1-\rho^2}}\right) = \big\{\textit{thanks to the symmetry of the Gaussian distribution}\big\} = \\
&= \mathcal{N}\left(\frac{\left(r_1-\frac{1}{2}\sigma_1^2\right)t+\rho w_2\sigma_1}{\sigma_1\cdot\sqrt{t}\cdot\sqrt{1-\rho^2}}\right)
\end{aligned}$$

To simplify the notation, we can define $d_2 = \frac{\left(r_1-\frac{1}{2}\sigma_1^2\right)t+\rho w_2\sigma_1}{\sigma_1\cdot\sqrt{t}\cdot\sqrt{1-\rho^2}}$ and we can write:

$$\mathbb{E}_0\Big[\mathbb{I}_{W_1(t)>-\frac{\left(r_1-\frac{1}{2}\sigma_1^2\right)t}{\sigma_1}}\Big|W_2(t)=w_2\Big] = \mathcal{N}(d_2) \qquad (43)$$

We can now compute the first expectation in (42):

$$\begin{aligned}
&\mathbb{E}_0\Big[S_1(t)\cdot\mathbb{I}_{W_1(t)>-\frac{\left(r_1-\frac{1}{2}\sigma_1^2\right)t}{\sigma_1}}\Big|W_2(t)=w_2\Big]=\big\{\textit{using the dynamics of } S_1(t)\big\}=\\
&=\mathbb{E}_0\Big[S_1(0)\cdot\exp\big\{(r_1-\frac{1}{2}\sigma_1^2)t+\sigma_1W_1(t)\big\}\cdot\mathbb{I}_{W_1(t)>-\frac{\left(r_1-\frac{1}{2}\sigma_1^2\right)t}{\sigma_1}}\Big|W_2(t)=w_2\Big]=\\
&=\big\{\textit{using Proposition 9.1 and taking out the deterministic quantities}\big\}=\\
&=S_1(0)\cdot\exp\big\{(r_1-\frac{1}{2}\sigma_1^2)t\big\}\cdot\\
&\cdot\mathbb{E}_0\Big[\exp\big\{\sigma_1(\rho W_2(t)+\sqrt{1-\rho^2}B_1(t))\big\}\cdot\mathbb{I}_{\rho W_2(t)+\sqrt{1-\rho^2}B_1(t)>-\frac{\left(r_1-\frac{1}{2}\sigma_1^2\right)t}{\sigma_1}}\Big|W_2(t)=w_2\Big]=\\
&=S_1(0)\cdot\exp\big\{(r_1-\frac{1}{2}\sigma_1^2)t+\sigma_1\rho w_2\big\}\int_{\frac{-\left(r_1-\frac{1}{2}\sigma_1^2\right)t-\rho w_2\sigma_1}{\sigma_1\cdot\sqrt{1-\rho^2}}}^{\infty}\Big[\exp\big\{\sigma_1\sqrt{1-\rho^2}\cdot s\big\}\cdot\frac{\exp\big\{-\frac{s^2}{2t}\big\}}{\sqrt{2\pi t}}\Big]ds=\\
&=\Big\{\textit{using the definition of } d_2\Big\}=\\
&=S_1(0)\cdot\exp\big\{(r_1-\frac{1}{2}\sigma_1^2)t+\sigma_1\rho w_2\big\}\int_{-d_2\sqrt{t}}^{\infty}\Big[\frac{1}{\sqrt{2\pi t}}\exp\Big\{-\frac{-2t\sigma_1\sqrt{1-\rho^2}\cdot s+s^2}{2t}\Big\}\Big]ds=\\
&=\big\{\textit{by adding and subtracting } \frac{1}{2}\sigma_1^2(1-\rho^2)t \textit{ at the argument of the exponential inside the integral}\big\}=\\
&=S_1(0)\cdot\exp\big\{(r_1-\frac{1}{2}\sigma_1^2)t+\sigma_1\rho w_2\big\}\cdot\\
&\cdot\int_{-d_2\sqrt{t}}^{\infty}\Big[\frac{1}{\sqrt{2\pi t}}\exp\Big\{-\frac{s^2-2t\sigma_1\sqrt{1-\rho^2}\cdot s+\sigma_1^2(1-\rho^2)t^2}{2t}+\frac{1}{2}\sigma_1^2(1-\rho^2)t\Big\}\Big]ds=\\
&=S_1(0)\cdot\exp\big\{(r_1-\frac{1}{2}\sigma_1^2)t+\sigma_1\rho w_2+\frac{1}{2}\sigma_1^2(1-\rho^2)t\big\}\int_{-d_2\sqrt{t}}^{\infty}\Big[\frac{1}{\sqrt{2\pi t}}\exp\Big\{-\frac{(s-t\sigma_1\sqrt{1-\rho^2})^2}{2t}\Big\}\Big]ds=\\
&=\Big\{\textit{simplify the exponent outside the integral and change of variable}:\ y=\frac{s-t\sigma_1\sqrt{1-\rho^2}}{\sqrt{t}}\Big\}=\\
&=S_1(0)\cdot\exp\big\{r_1t+\sigma_1\rho w_2-\frac{1}{2}\sigma_1^2\rho^2t\big\}\int_{-d_2-\sigma_1\sqrt{t}\cdot\sqrt{1-\rho^2}}^{\infty}\Big[\frac{1}{\sqrt{2\pi}}\exp\Big\{-\frac{y^2}{2}\Big\}\Big]dy=\\
&=S_1(0)\cdot\exp\big\{r_1t+\sigma_1\rho w_2-\frac{1}{2}\sigma_1^2\rho^2t\big\}\Big(1-\mathcal{N}\Big(-d_2-\sigma_1\sqrt{t}\cdot\sqrt{1-\rho^2}\Big)\Big)=\\
&=S_1(0)\cdot\exp\big\{r_1t+\sigma_1\rho w_2-\frac{1}{2}\sigma_1^2\rho^2t\big\}\mathcal{N}\Big(d_2+\sigma_1\sqrt{t}\cdot\sqrt{1-\rho^2}\Big)
\end{aligned}$$

We can define $d_1=\frac{\left(r_1-\frac{1}{2}\sigma_1^2\right)t+\rho w_2\sigma_1}{\sigma_1\cdot\sqrt{t}\cdot\sqrt{1-\rho^2}}+\sigma_1\sqrt{t}\cdot\sqrt{1-\rho^2}=d_2+\sigma_1\sqrt{t}\cdot\sqrt{1-\rho^2}$, hence we get:

$$\mathbb{E}_0\Big[S_1(t)\cdot\mathbb{I}_{W_1(t)>-\frac{\left(r_1-\frac{1}{2}\sigma_1^2\right)t}{\sigma_1}}\Big|W_2(t)=w_2\Big]=S_1(0)\cdot\exp\big\{r_1t+\sigma_1\rho w_2-\frac{1}{2}\sigma_1^2\rho^2t\big\}\cdot\mathcal{N}\big(d_1\big)\tag{44}$$

By substitution of (43) and (44) in (42), we obtain:

$$\mathbb{E}_0\Big[(S_1(t)-S_1(0))^+\Big|W_2(t)=w_2\Big]=S_1(0)\cdot\Big\{\exp\big\{r_1t+\sigma_1\rho w_2-\frac{1}{2}\sigma_1^2\rho^2t\big\}\cdot\mathcal{N}\big(d_1\big)-\mathcal{N}\big(d_2\big)\Big\}\tag{45}$$

We can finally plug this result in equation (41), and we obtain the expression for the semi-closed formula:

$$\mathbb{E}_0\Big[D_1(0,t)\cdot(S_1(t)-S_1(0))^+\cdot\mathbb{I}_{S_2(t)<0.95\cdot S_2(0)}\Big]=$$

$$=\bar{B}_1(0,t)\cdot S_1(0)\cdot\int_{-\infty}^{\frac{ln(0.95)-(r_2-\frac{1}{2}\sigma_2^2)t}{\sigma_2}}\Big\{\exp\big\{r_1t+\sigma_1\rho w_2-\frac{1}{2}\sigma_1^2\rho^2t\big\}\cdot\mathcal{N}\big(d_1\big)-\mathcal{N}\big(d_2\big)\Big\}f_{W_2}(w_2)dw_2 \qquad (46)$$

$$\text{where}\quad d_1=\frac{\big(r_1-\frac{1}{2}\sigma_1^2\big)t+\rho w_2\sigma_1}{\sigma_1\cdot\sqrt{t}\cdot\sqrt{1-\rho^2}}+\sigma_1\sqrt{t}\cdot\sqrt{1-\rho^2}\qquad\text{and}\quad d_2=d_1-\sigma_1\sqrt{t}\cdot\sqrt{1-\rho^2}$$

As previously observed, it is difficult to explicitly solve this integral, since in the integrand there is the product of the Gaussian density function $f_{W_2}(w_2)$ and of the normal cumulative distribution function in function of the integration variable w (i.e. $\mathcal{N}(d_1)$ or $\mathcal{N}(d_2)$).
Luckly, the integral in the semi-closed formula can be solved via different numerical methods, as the adaptive quadrature method that we choose, in order to have efficient and accurate integration results.

This semi-closed formula can be also retrieved by a different approach: instead of using Proposition 9.1, we can exploit the properties of conditioned Gaussian vectors, according to the following proposition.

Proposition 9.2:
Given a two dimensioned Gaussian vector:

$$\big(X,Y\big)\sim\mathcal{N}\left(\begin{bmatrix}\mu_X\\ \mu_Y\end{bmatrix},\begin{bmatrix}\sigma_X^2 & \rho\sigma_X\sigma_Y\\ \rho\sigma_X\sigma_Y & \sigma_Y^2\end{bmatrix}\right)$$

if $\sigma_X>0$, we have that $X|Y=s\sim\mathcal{N}(m(s),q^2)$, where

$$m(s)=\mathbb{E}[X|Y=s]=\mu_X+\frac{COV(X,Y)}{Var(Y)}(s-\mu_Y)=\mu_X+\rho\frac{\sigma_X}{\sigma_Y}(s-\mu_Y)$$
$$q^2=Var(X|Y=s)=Var(X)-\frac{COV(X,Y)}{Var(Y)}=\sigma_X^2(1-\rho^2)$$

By applying this proposition to the correlated Brownian Motions $(W_1(t),W_2(t))$, we get:

$$W_1(t)\mid W_2(t)=w\sim\mathcal{N}\big(\rho w,t(1-\rho^2)\big)$$

This alternative approach can be used in equation (42) to compute the conditional expectations; however, the computations are omitted since we get to the same semi-closed formula result obtained in (46).

The price obtained by applying this semi-closed formula is reported in Table 10.

9.5 Derivative product prices

Method	Price [$]	CI [$]	Calibration time [sec]	Pricing time [sec]
Levy model	81.8512	[81.7048 ; 81.9976]	101.66	3.2196
Levy model AV	81.8114	[81.6650 ; 81.9577]	101.66	3.2196
Levy semi-closed	81.8294	-	-	0.4738
Black model	14.7530	[14.7033 ; 14.8027]	0.9019	0.7120
Black model AV	14.7762	[14.7264 ; 14.8260]	0.9019	0.7120
Black semi-closed	14.7664	-	-	0.0132

Table 10: Derivative's price, confidence interval of the price, and computational time for different methods. For all the Monte-Carlo simulations 10 000 000 are used.

From this table we observe that the Levy model and the Black model yield different results.

The different approaches implemented to price the derivative via the Black model agree that the price falls in the interval $[14.7\,\$; 14.8\,\$]$. From this result, we could infer that the semi-closed formula retrieved in the previous section is correct and it also has the advantage to have a significantly lower computational time.

The Levy model price is 81.8512 $, it is higher than the Black one: this discrepancy is quite large but it can be explained as follows. In fact we are calibrating among a multitude of maturities which lead us into not reaching the desired market correlation.

Moreover our contract's payoff highly depends on the correlation between the two markets: in order to obtain a high payoff, the general buyer would like the USA market to rise and instead the European market to decrease. This is more likely to happen if there is a low correlation between the markets; in this way the underlying are more prone to move in desired direction and guarantee a higher payoff.

In our case the market correlation, which is well captured by Black's model, is relatively high and therefore there are less cases in which we have a positive payoff.

The Levy model we calibrated sacrificed precision on the correlation in order to correctly capture volatility and market prices and, for this reason, we have a higher price then the one computed via Black.

It is important to know that even thought the prices computed are higher then what we expected, we still believe that they should be larger than the ones computed by Black since Levy model captures better, thanks to its parameters, skewness and symmetry of the market and therefore manage the risk in a more precise way.

In order to improve the Levy model, we could implement another minimization method that can find more precisely the global minimum of the objective function and match better the historical correlation. We believe that the structure of our code is solid and that with more powerful tools we would be able to correctly price exotic contracts.

10 Conclusions

In this case study we were asked to consider various shades of the equity world: we considered a elaborate process composed by both idiosyncratic and systematic risk components that lie implicitly in the two markets we examined, the S&P500 and the EUROSTOXX50, following Ballotta & Bonfiglioli, 2016 procedure. Moreover we priced a derivative contract with different methods, comparing and analyzing the results.

To obtain the discount factors and the forward prices that we used through out the project we followed the procedure described by Baviera & Azzone, 2021 which resulted to be an effective and practical way to obtain implicit discount factors.

Levy The multivariate Levy process is described entirely by its characteristic function: the structure that supports it is the one described by an alpha tempered stable model. In our case we were asked to operate in a framework with $\alpha = \frac{1}{2}$ and therefore with a Normal Inverse Gaussian (NIG) process.

The first step of our case study was to show how by starting from a model

$$X = (X_1, X_2) = (Y_1 + a_1 \cdot Z,\ Y_2 + a_2 \cdot Z)$$

where Y and Z are NIG processes, we still obtained a multivariate NIG.

Having found this, we derived an expression for the drift compensator (p_i) which ensured the martingality of the forward prices

$$F_i(t,T) = F_i(t_0,T) \cdot e^{p_i \cdot t + X_i(t)}$$

Moreover we computed the correlation between the two components of the multivariate Levy and proceeded with a two step calibration. First of all, we calibrated separately the six parameters of the two marginals X_i with put and call prices; afterwards, we proceeded by calibrating the idiosyncratic components Y_i and the common term Z on the historical correlation.

At this point we had all the parameters needed for the pricing of a contract. In our case we priced an exotic derivative: $(S_1(t) - S_1(0))^+ \cdot \mathbb{I}_{S_2(t) < 0.95 \cdot S_2(0)}$

Black As a term of comparison we calibrated the Black model on the same market data by computing the Black volatility and we proceeded by pricing the same contract.

Comparison between the two models: Let's take now a deeper dive into the differences between this to models:

- The **Black model** has only one parameter that needs calibration, this guarantees a faster and parsimonious approach which although lacks in terms of precision and correctness of the prices obtained.

  Moreover, since we have an unique volatility value that needs to fit multiple strikes and expiries, we are not able to model correctly the skewness of the volatility smiles and the "vol o vol". As a good note Black's model is able to match correctly the model correlation with the one derived from the market.

- The **Levy Model** is more onerous since it adds many parameters to resolve the simplistic approach taken by Black. It has a more precise description of the volatility smiles and of the prices computed with it. As a result of the added explanatory power we obtain a computationally onerous and time demanding calibration.

  The results capture a snapshot of the market and describe correctly its volatility by representing the equity skewness and the "vol of vol". Unfortunately, due to the added parameters and to the constraints between them we are not able to match the historical correlation differently from Black's model case.

11 Appendix 1: Dataset exploration

The initial dataset requires an obligatory exploration of its components in order to ensure that there is neither human mistake in the table creation nor conversions discrepancies for the scale measurements.

The dataset is composed by different time maturities; the starting date is set on July 9^{th} 2023 meanwhile the prices cover a long period: American data end on December 15^{th} 2028 and Europeans on June 20^{th} 2025. Each maturity contains multiple structures describing call and put bid/ask prices, strikes, the initial spot price and the trading volumes that describe the liquidity of the assets.

At first, following the indications of the Azzone & Baviera, 2021 paper, we verify that there are not **Penny options**, hence those options whose value is lower than 0.1 index points, and that the liquidity criteria for the Ask/Bid spread is verified.

Let's start the description through the comparison of the prices over all the maturities for all the markets. We noticed that the strikes are increasing in number and range as long as the maturity is far away from the settlement date:

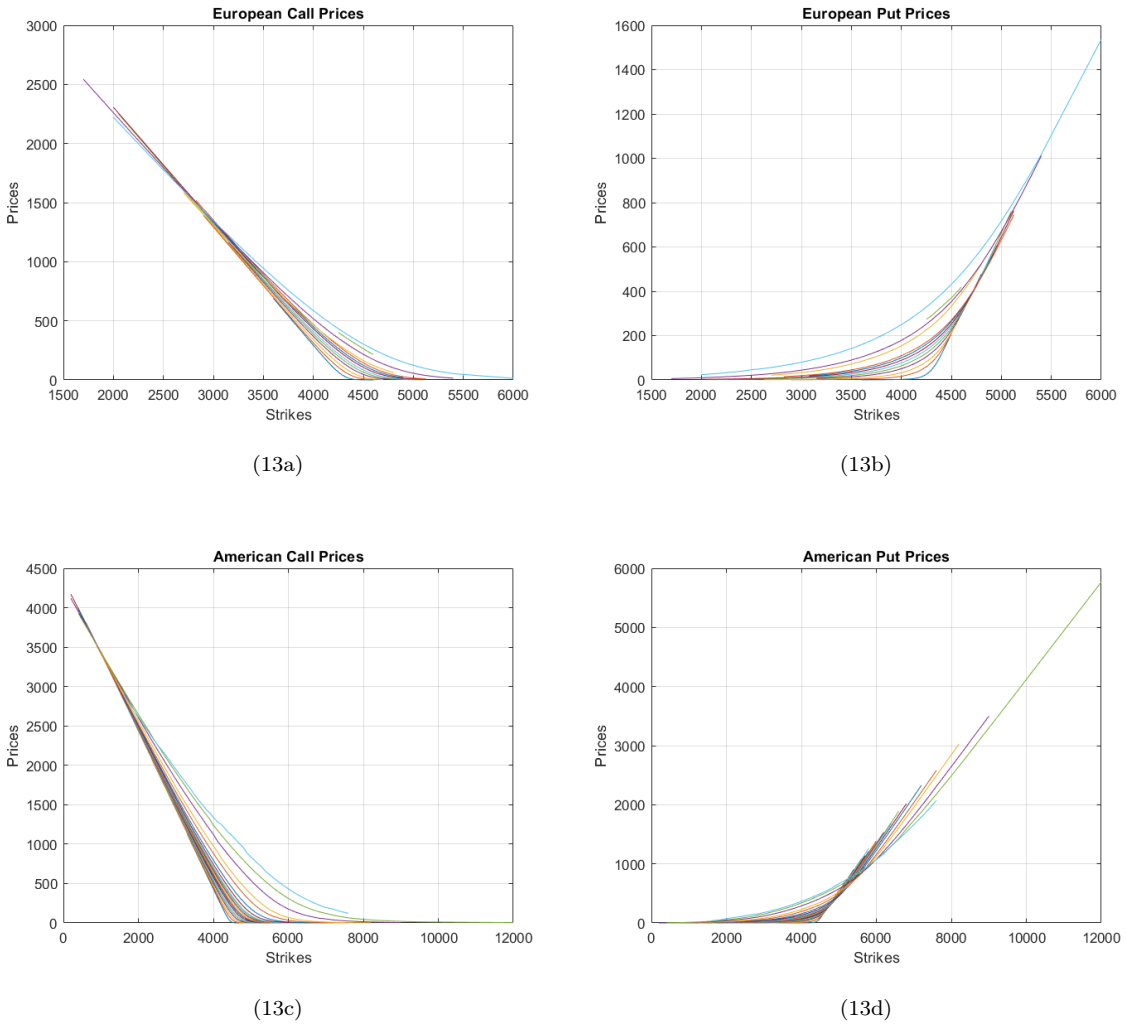

(13a) (13b)

(13c) (13d)

Figure 13: Mid prices for European Call options (13a), European Put Options (13b), American Call Options (13c), and American Put Options (13d).

The prices plots have a few differences due to the structure of the S&P500 and the EUROSTOXX50 markets:

- The prices of the **In The Money options** (ITM) are quite different from each other as a consequence of the implied volatility size. The American market has a larger volatility than the European one; hence the prices, that can be exploited starting from the same underlying stock, are higher.

- The **strikes** considered for the prices **have a larger range** in the USA market and a more detailed grid discretization; this can simplify the computational structure since the curve is smoother and less piece wise interpolated.

The only similarity between the two markets fall on the choice of the At The Money (ATM) strike over the curve; in both cases this particular point is between 4000 and 4500. We need to compare these assumptions with respect to the ones computed through the Synthetic Forward procedure since we expect them to be coherent with each other.

Sadly the true results are a bit disappointing; the Forward values extrapolated from the market move way over the hypothetical threshold of 5000. Moreover their behaviour is not strictly increasing, as we would expect from the theory, but it has a broken pattern for the EU market:

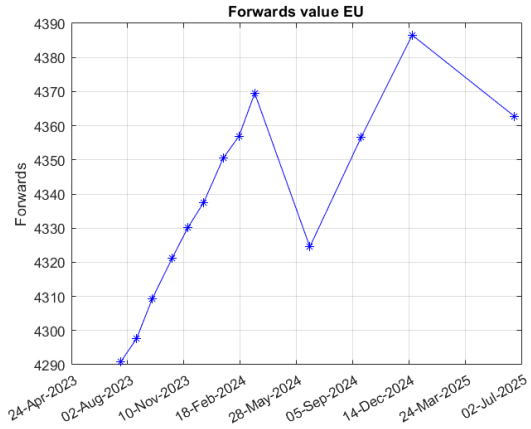

(14a)

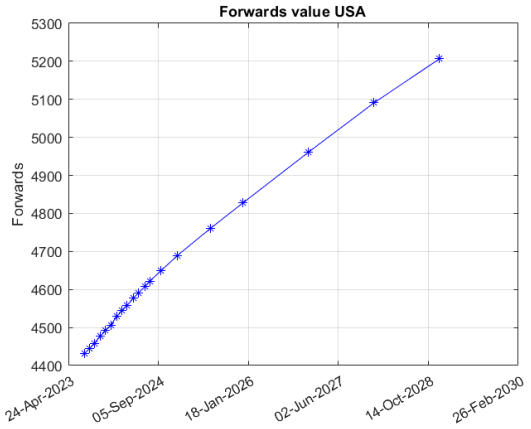

(14b)

Figure 14: Forward prices obtained via the synthetic forwards procedure for the European market (14a) and for the American market (14b).

In order to better visualize the theoretical behaviour of the initial forward value $F(t_0, t_i)$, we decided to extrapolate the continuously compounded interest rates from the discount factors and then apply the *Garman - Kholhagen* formula to get the forward value:

Garman - Kholhagen $$F(t_0, t_i) = S_0 \cdot e^{r \cdot (t_i - t_0)}$$

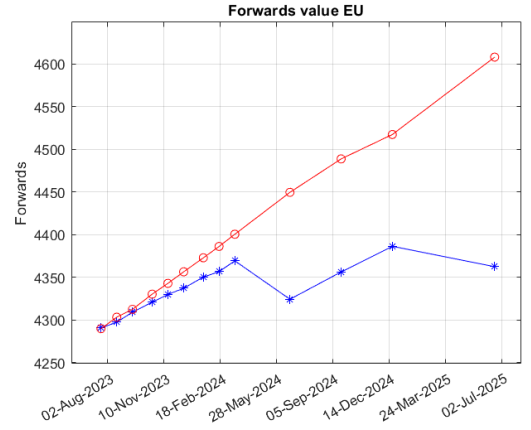

(15a)

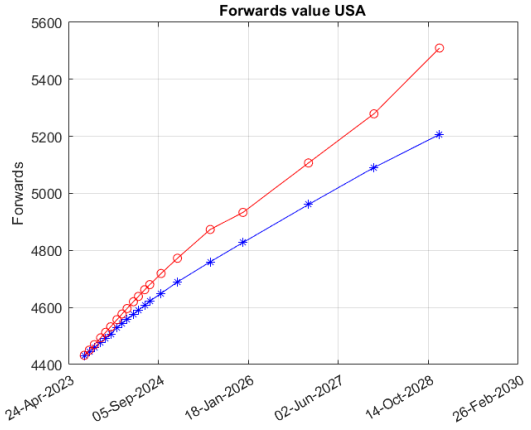

(15b)

Figure 15: Forward prices obtained via the synthetic forwards procedure (blue lines) and extrapolated forwards from the discounts via the Galman - Kholhagen formula (red lines) for the European market (15a) and for the American market (15b).

As it's possible to see, the EU Forward values are divergent with respect to the theoretical description from Garman - Kholhagen meanwhile the American ones can be considered equal; it's obvious that the two curves

don't match but we can take it as a consequence of the Synthetic Forward procedure.

Financial Interpretation The European forwards curve obtained via the synthetic forwards procedure seem to have a strange not-monothonic behaviour, which could be due to different factors; however, a shareable interpretation is that the market prices of the Put and the Call options reflect the market expectations, and in particular the interest rates expectations.

In the given dataset we are considering the market data at the 9^{th} of July 2023: at that time the European Central Bank had already raised the interest rates four times from the start of the year, and there was an high expectation for other rises (see the Financial Times 27^{th} June 2023 article), which impacted the prices of the options with shorter expires. On the other hand, the rates were expected to be cut from the start of the 2024, which had an impact over options with longer expires.

11.1 Surface vols

We decided to plot the surface of the implied market volatility's in order to have a larger and more comprehensive view on the behaviour of our dataset.

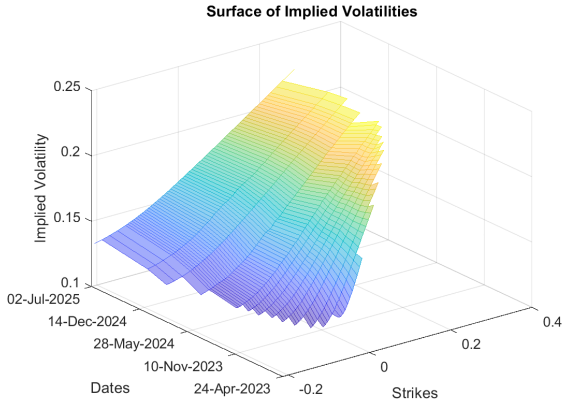

Figure 16: European market

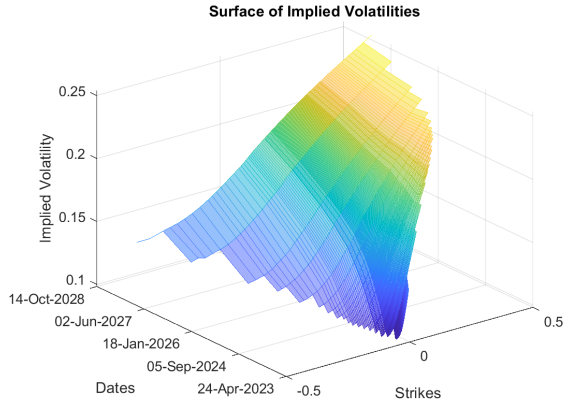

Figure 17: American market

In the structure provided some implied vols for OTM strikes and distant maturity's where missing, for visualization purposes, we decided to extrapolate on the missing values.

12 Appendix 2: Forward prices interpretation

The forwards prices are the building block for the multivariate Levy pricing and they need to be studied deeply in order to tackle eventual outliers in the datasets. The exploration of the forward values was divided in two main parts related to the market that they were representing, studying the different maturities in a temporal increasing order.

EUROSTOXX50

The European EUROSTOXX50 is a stable and important market that doesn't allow too many fluctuations around its mid prices; therefore the forwards should be constant around a specific value for each of the maturities considered.

Let's represent the European Forward prices for some relevant maturities:

As the above plots show, the previous assumptions of stability were highly satisfied for the first year after the settlement date. The shortest maturity exhibit a peculiar behaviour around the ATM point since the value of both bid and ask prices collapse toward a single point. It's due to the absence of the intrinsic value of the option

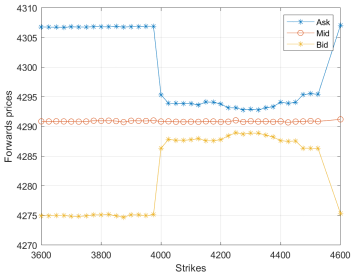

(18a): expiry 2023-07-21

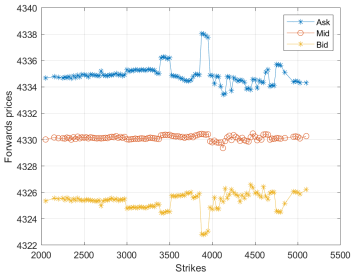

(18b): expiry 2023-11-17

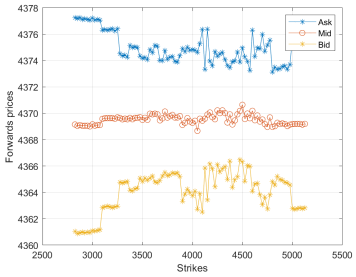

(18c): expiry 2024-03-15

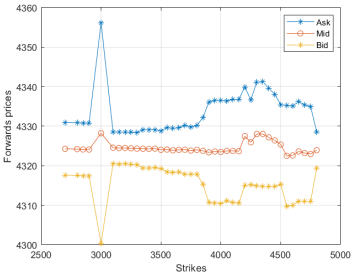

(18d): expiry 2024-06-21

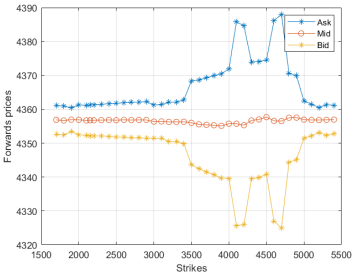

(18e): expiry 2024-09-20

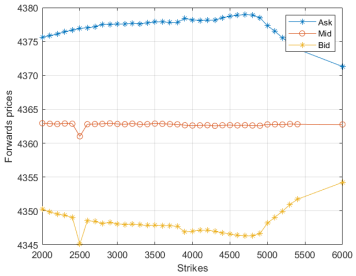

(18f): expiry 2025-06-20

Figure 18: European forward prices for some relevant maturities.

around the specified point; the value of the option is similar to the one of the underlying which means that the profit is deriving only from the stochastic time value of the option.

The second row of plots display an unusual behaviour with respect the previous ones since they do not shrink anymore around the ATM point, instead they tend to enlarge their range of values.

S&P500

The American market is more unstable than the European one due to the higher volatility of the contracts and the greater propensity of the traders to enter into a risky contract. This behaviour can be highly seen in the last maturities shown below where the forwards prices are spread along a wide range; moreover the shrinkage at the ATM point is no more displayed for long time contracts.

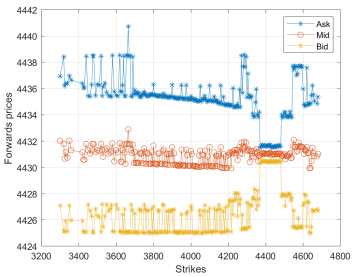

(19a): expiry 2023-07-21

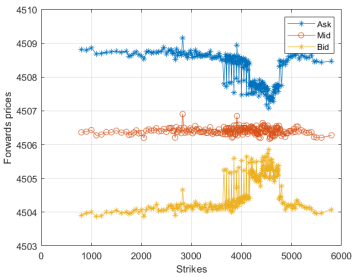

(19b): expiry 2023-12-15

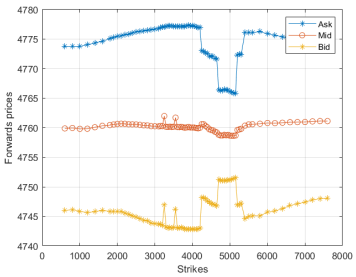

(19c): expiry 2025-12-19

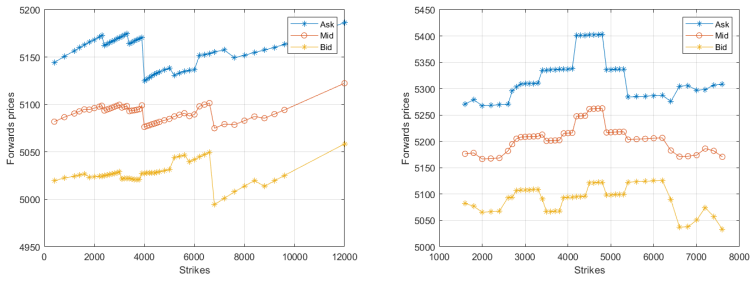

(19d): expiry 2027-12-17 (19e): expiry 2028-12-15

Figure 19: American forward prices for some relevant maturities.

13 Appendix 3: Multiple calibration

The multiple calibration procedure is a customized method created to justify in a rigorous way the maturities chosen for the marginal parameters calibration. The method is quite simple; it repeats a joint calibration procedure removing each time a single maturity from the European or American market. Consequently we compared the weighted RMSE obtained as final objective value function and discuss about the results.

13.1 First multi-calibration

The first multi-calibration starts from the most general framework pre-processed in Section 6 and tries to detect the worst maturity among all the available ones.

The result obtained from this procedure are summarized in the following table:

EU Date removed	κ_{USA}	θ_{USA}	σ_{USA}	κ_{EU}	θ_{EU}	σ_{EU}	(w)RMSE
21/07/2023	3.3692	-0.0967	0.1519	0.8602	-0.1586	0.1259	365.5763
18/08/2023	3.3304	-0.0982	0.1503	0.0100	1.1955	0.1003	508.0701
15/09/2023	3.3301	-0.0982	0.1503	0.0100	1.1957	0.1003	505.7878
20/10/2023	3.3299	-0.0982	0.1503	0.0100	1.1956	0.1003	503.6564
17/11/2023	0.0100	1.1040	0.1118	1.1717	-0.1285	0.1409	715.8963
15/12/2023	0.0100	1.1036	0.1119	1.1781	-0.1282	0.1411	716.4983
19/01/2024	0.0100	1.1008	0.1122	1.1793	-0.1279	0.1415	717.2743

Table 11: Parameters European removal pt1

EU Date removed	κ_{USA}	θ_{USA}	σ_{USA}	κ_{EU}	θ_{EU}	σ_{EU}	(w)RMSE
16/02/2024	3.3618	-0.0970	0.1516	0.8973	-0.1566	0.1264	369.1801
15/03/2024	3.3603	-0.0970	0.1515	0.7851	-0.1647	0.1243	369.2498
21/06/2024	3.3640	-0.0969	0.1517	0.7551	-0.1668	0.1237	367.4005
20/09/2024	3.3629	-0.0969	0.1516	0.7504	-0.1672	0.1236	366.3818
20/12/2024	3.3665	-0.0968	0.1518	0.8382	-0.1608	0.1259	367.3232
20/06/2025	3.3301	-0.0982	0.1503	0.0100	1.1855	0.0995	489.6617

Table 12: Parameters European removal pt2

USA Date removed	κ_{USA}	θ_{USA}	σ_{USA}	κ_{EU}	θ_{EU}	σ_{EU}	(w)RMSE
21/07/2023	3.3519	-0.0980	0.1505	0.0100	1.1934	0.1001	511.6416
18/08/2023	3.4055	-0.0966	0.1520	0.8378	-0.1605	0.1253	365.2853
15/09/2023	3.3775	-0.0981	0.1504	0.0100	1.1955	0.0998	510.4104
20/10/2023	3.4003	-0.0979	0.1506	0.0100	1.1958	0.0998	510.9049
17/11/2023	3.3948	-0.0981	0.1504	0.0100	1.1970	0.0996	510.9426
15/12/2023	3.4015	-0.0981	0.1504	0.0100	1.1974	0.0996	511.0459
19/01/2024	3.3876	-0.0983	0.1504	0.0100	1.1976	0.0995	511.3730

Table 13: Parameters American Removal pt1

USA Date removed	κ_{USA}	θ_{USA}	σ_{USA}	κ_{EU}	θ_{EU}	σ_{EU}	(w)RMSE
16/02/2024	3.4133	-0.0981	0.1506	0.0100	1.1975	0.0996	511.6331
15/03/2024	3.4299	-0.0980	0.1507	0.0100	1.1977	0.0995	512.0059
19/04/2024	3.4512	-0.0978	0.1510	0.0100	1.1974	0.0996	512.4030
17/05/2024	3.4780	-0.0974	0.1513	0.0100	1.1966	0.0997	512.8118
21/06/2024	3.4862	-0.0971	0.1517	0.0100	1.1946	0.0999	513.1567
19/07/2024	3.4909	-0.0969	0.1519	0.0100	1.1931	0.1001	513.3363
20/09/2024	3.4772	-0.0966	0.1522	0.0100	1.1894	0.1005	513.7457

Table 14: Parameters American Removal pt2

USA Date removed	κ_{USA}	θ_{USA}	σ_{USA}	κ_{EU}	θ_{EU}	σ_{EU}	(w)RMSE
20/12/2024	3.2833	-0.0969	0.1514	0.0100	1.1797	0.1017	513.2031
20/06/2025	3.1167	-0.0986	0.1495	0.0100	1.1812	0.1015	511.3846
19/12/2025	3.0954	-0.0986	0.1496	0.0100	1.1793	0.1017	508.7120
18/12/2026	2.8710	-0.1011	0.1466	0.0100	1.1835	0.1012	503.2580
17/12/2027	2.6618	-0.1037	0.1439	0.0100	1.1864	0.1009	494.9451
15/12/2028	3.8295	-0.0941	0.1558	0.8259	-0.1621	0.1246	119.2546

Table 15: Parameters American Removal pt3

Looking at the weighted RMSE can give us a double hint over the choices to make: from one hand the highest (w)RMSE discovered remark the importance of some dates over the calibration, on the other side the lowest (w)RMSE traces a clear path to the date removal.

Therefore excluding the last American maturity from the calibration, as shown in the previous tables, leads to a lower final objective function value, resulting in a better outcome. In support to this outcome, the following plots show the objective function behaviour over the dates considered:

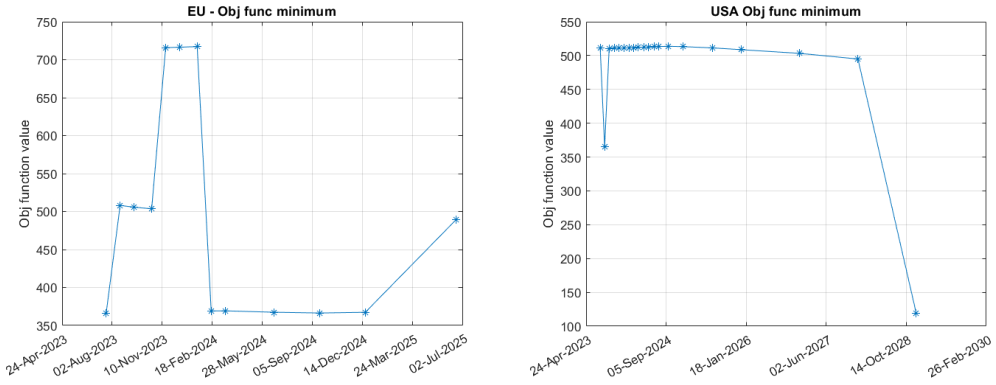

(20a) (20b)

Figure 20: European (20a) and American (20b) Objective function minimum for marginal calibration value by excluding one expiry at a time in the first step of the multi-calib procedure.

13.2 Second multi-calibration

The second multi-calibration starts from the first step results and recompute again the procedure aiming to find further dates to discard from the dataset. Also in this framework, the result obtained can be studied from the following tables:

EU Date removed	κ_{USA}	θ_{USA}	σ_{USA}	κ_{EU}	θ_{EU}	σ_{EU}	(w)RMSE
21/07/2023	3.8287	-0.0942	0.1557	0.8417	-0.1610	0.1248	114.9621
18/08/2023	3.8277	-0.0942	0.1557	0.8554	-0.1600	0.1250	114.8493
15/09/2023	0.0100	1.1225	0.1135	1.1469	-0.1297	0.1404	483.7710
20/10/2023	3.8271	-0.0942	0.1557	0.8749	-0.1587	0.1253	116.2545
17/11/2023	3.8274	-0.0942	0.1557	0.8826	-0.1581	0.1255	116.7358
15/12/2023	3.7932	-0.0956	0.1542	0.0100	1.2013	0.0995	250.3505
19/01/2024	3.7932	-0.0956	0.1542	0.0100	1.2017	0.0995	249.0813

Table 16: Parameters European removal pt1

EU Date removed	κ_{USA}	θ_{USA}	σ_{USA}	κ_{EU}	θ_{EU}	σ_{EU}	(w)RMSE
16/02/2024	3.7932	-0.0956	0.1542	0.0100	1.2008	0.0994	248.1029
15/03/2024	3.7931	-0.0956	0.1542	0.0100	1.2008	0.0994	247.0922
21/06/2024	3.7933	-0.0956	0.1542	0.0100	1.1953	0.0990	244.8194
20/09/2024	3.7931	-0.0956	0.1542	0.0100	1.1977	0.0992	242.9225
20/12/2024	3.8267	-0.0942	0.1556	0.8210	-0.1632	0.1248	116.6985
20/06/2025	3.7935	-0.0956	0.1542	0.0100	1.1918	0.0987	238.8963

Table 17: Parameters European removal pt2

USA Date removed	κ_{USA}	θ_{USA}	σ_{USA}	κ_{EU}	θ_{EU}	σ_{EU}	(w)RMSE
21/07/2023	3.8536	-0.0941	0.1559	0.8231	-0.1625	0.1244	115.7649
18/08/2023	3.8384	-0.0954	0.1543	0.0100	1.2010	0.0991	259.5791
15/09/2023	3.8517	-0.0954	0.1543	0.0100	1.2018	0.0990	259.4804
20/10/2023	3.8798	-0.0953	0.1545	0.0100	1.2022	0.0990	259.9090
17/11/2023	3.9066	-0.0941	0.1559	0.8137	-0.1637	0.1238	114.9489
15/12/2023	3.8754	-0.0955	0.1543	0.0100	1.2037	0.0988	259.9848
19/01/2024	3.8566	-0.0957	0.1542	0.0100	1.2037	0.0988	260.2928

Table 18: Parameters American Removal pt1

USA Date removed	κ_{USA}	θ_{USA}	σ_{USA}	κ_{EU}	θ_{EU}	σ_{EU}	(w)RMSE
16/02/2024	3.8848	-0.0955	0.1545	0.0100	1.2037	0.0988	260.4801
15/03/2024	3.9024	-0.0954	0.1546	0.0100	1.2040	0.0988	260.7993
19/04/2024	3.9251	-0.0952	0.1549	0.0100	1.2037	0.0988	261.1296
17/05/2024	3.9546	-0.0950	0.1552	0.0100	1.2033	0.0988	261.4936
21/06/2024	3.9646	-0.0948	0.1555	0.0100	1.2019	0.0990	261.8329
19/07/2024	3.9744	-0.0946	0.1557	0.0100	1.2011	0.0991	261.9991

Table 19: Parameters American Removal pt2

USA Date removed	κ_{USA}	θ_{USA}	σ_{USA}	κ_{EU}	θ_{EU}	σ_{EU}	(w)RMSE
20/09/2024	3.9974	-0.0944	0.1560	0.0100	1.2001	0.0992	262.4371
20/12/2024	3.9659	-0.0932	0.1570	0.0100	1.1891	0.1006	262.6300
20/06/2025	3.6614	-0.0950	0.1546	0.0100	1.1865	0.1009	261.4888
19/12/2025	0.0100	1.1172	0.1130	1.0878	-0.1323	0.1396	449.9594
18/12/2026	3.3644	-0.0961	0.1526	0.8600	-0.1577	0.1266	109.0638
17/12/2027	3.1082	-0.0984	0.1497	0.8550	-0.1583	0.1263	101.6791

Table 20: Parameters American Removal pt3

Once again the tables can give us an overview of the general behaviour of the calibration: after the removal of the last American maturity the evaluation errors highly changed, showing a more similar conduct among the time grid.

The only result, which is valuable to be shown, is the second-to-last American maturity with the lowest value of (w)RMSE; however we're reluctant to remove it since it can easily collapse the model into overfitting. The evaluation errors can be better displayed through the following graphs:

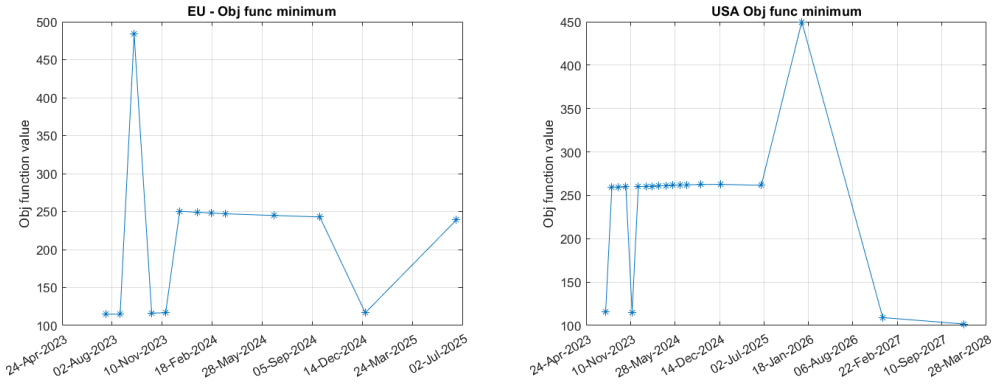

(21a) (21b)

Figure 21: European (21a) and American (21b) Objective function minimum for marginal calibration value by excluding one expiry at a time in the second step of the multi-calibration procedure.

14 Appendix 4: Python

We decided to implement a Python version of the code, reducing the steps to the essential in order to have an idea of how the approaches chosen work on a different environment.

The Python code tries to exploit the main environmental differences between Python and MATLAB; the most important feature is the possibility to create an **object oriented framework** to encode the project. The OOP is commonly used to deal with repetitive objects inside the dataset; therefore we introduced it to represent the data structure in a more efficient and accessible way. The other functionalities of the project were summed up in multiple levels of libraries, divided in the relative work sections.

The backbone of the project remains the same, the steps are similar and the customized functions are only a transposition of the MATLAB code into the Python language. Nevertheless the main built-in procedure or functions like *fmincon, fsolve, ...* were not implemented, hence we needed to find a substitute method for the calibration solvers: in the Python environment are inserted more advanced algorithms for function minimization and root solving.

There were two main method used to replace the solvers of MATLAB:

- **Sequential Least Squares Quadratic Programming (SLSQP)**: it is an optimization method for solving nonlinear optimization problems. It's particularly well-suited for problems with constraints, including equality and inequality constraints; therefore it over take the *fmincon* function with the non linear constraint:

$$\frac{\sigma_1^2}{k_1 \cdot \theta_1^2} = \frac{\sigma 2^2}{k_2 \cdot \theta_2^2}$$

- **Brent's method**: it's a robust and efficient root-finding algorithm that combines elements of the bisection method, the secant method, and inverse quadratic interpolation. We used it in order to compute the black volatilities for both Black and Lewis Call prices

The algorithm used are really different from the previous ones in MATLAB and more precise; therefore the calibrated result were slightly different from the previous ones:

	k	θ	σ
USA	3.2736	-0.0964	0.1524
EU	0.8150	-0.1602	0.1264

Table 21: Calibrated parameters for X.

	ν	β	γ
USA	7.8582	-0.0402	0.0984
EU	0.9535	-0.1370	0.1169

Table 22: Calibrated parameters for Y.

	ν	β	γ	a_{USA}	a_{EU}
Z	5.6110	0.3132	0.6482	-0.1796	-0.0743

Table 23: Calibrated parameters for Z

The main differences fall on the order of magnitude of the volvol; the American X_t volvol is reduced from before and consequently the idiosyncratic and systematic processes have their parameters reduced; however the constraints are still verified by the solvers

Following the same procedure as before, we decided to simulate the price of a Levy and a Black process from the new calibrated parameters. It's important to notice that the Black volatilities are the same even changing programming environment, therefore we suppose a similar final price. The prices obtained with the parameters are the following:

Method	Price [$]	CI [$]	Calibration time [sec]	Pricing time [sec]
Levy model	80.9028	[80.7569; 81.0486]	147.02	8.09
Black model	14.7658	[14.7161; 14.8155]	2.40	1.28

Table 24: Derivative's price, confidence interval of the price, and computational time for different methods.

As it can be seen the Black price remains coherent to the MATLAB one; instead, due to the different calibration procedure, the Levy price is quite different from the previous one but still higher than the Black Montecarlo procedure.

15 Appendix 5: Computational Time

This appendix has been created in order to show to the reader some insight over the computational time required by the processes used; we focused on the MATLAB time division since the Python is similar. The times and procedure shown in the report were computed using a computer with 16 GB of RAM and an Inteli7 processor; therefore different kinds of PC can lead to a different time management.

The following time chart show the MATLAB time division:

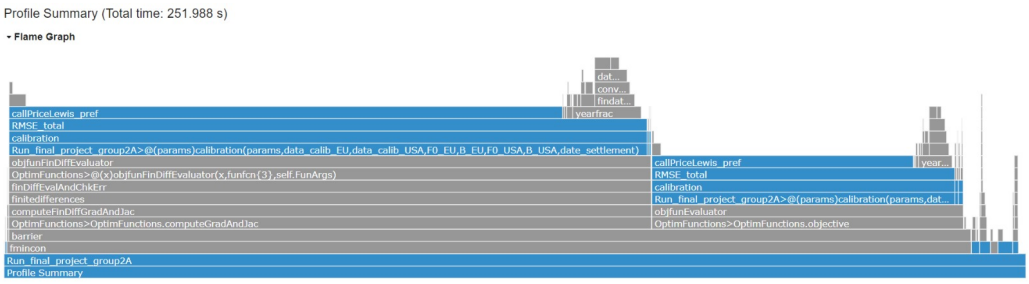

Figure 22: Run time

The most computationally onerous functions are:

- **callPriceLewis-pref**: this method appears to be the most time-consuming, occupying a significant portion of the total runtime. A similar result is obvious since the callLewis compute the Fast Fourier Transforms for each iteration of the calibrations
- **RMSE-total**: calculation of the Root Mean Square Error (RMSE) and used in the calibration procedure.
- **Calibration**: The main calibration function which contains the main steps of the first marginal parameters calibration

It is also important to notice that the same code ran on multiple architectures yields different results due to the internal structure of the CPU.

16 Bibliography

Books:

- **Cont R. & Tankov P. (2004)** Financial modelling for jump processes

Papers & Researches:

- **Laura Ballotta & Efrem Bonfiglioli (2016)** Multivariate asset models using Lévy processes and applications , The European Journal of Finance, 22:13, 1320-1350.
- **Michele Azzone, Roberto Baviera** Synthetic forwards and cost of funding in the equity derivative market.

Newspapers:

- ECB must persist with high rates to ward off wage-price spiral, says Christine Lagarde, Financial Times, 27th of June 2023.

POLITECNICO
MILANO 1863